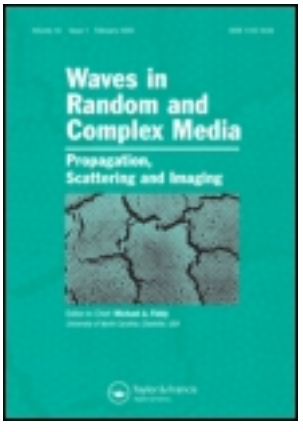

Waves in Random and Complex Media
Publication details, including instructions for authors and subscription information:
http://www.tandfonline.com/loi/twrm20

Enhanced and specular backscattering in random media

Maarten V. de Hoop [a], Josselin Garnier [b] & Knut Solna [c]

[a] Center for Computational and Applied Mathematics, Purdue University, 150 N. University Street, WestLafayette, IN 47907, USA

[b] Laboratoire de Probabilités et Modèles Aléatoires & Laboratoire Jacques-Louis Lions, Université Paris 7, Site Chevaleret 75205, Paris Cedex 13, France

[c] Department of Mathematics, University of California at Irvine, Irvine, CA 92697-3875, USA

Published online: 08 Nov 2012.

To cite this article: Maarten V. de Hoop , Josselin Garnier & Knut Solna (2012) Enhanced and specular backscattering in random media, Waves in Random and Complex Media, 22:4, 505-530, DOI: 10.1080/17455030.2012.728299

To link to this article: http://dx.doi.org/10.1080/17455030.2012.728299

Waves in Random and Complex Media
Vol. 22, No. 4, November 2012, 505–530

Enhanced and specular backscattering in random media

Maarten V. de Hoop[a], Josselin Garnier[b] and Knut Solna[c]*

[a]*Center for Computational and Applied Mathematics, Purdue University, 150 N. University Street, WestLafayette, IN 47907, USA;* [b]*Laboratoire de Probabilités et Modèles Aléatoires & Laboratoire Jacques-Louis Lions, Université Paris 7, Site Chevaleret 75205, Paris Cedex 13, France;* [c]*Department of Mathematics, University of California at Irvine, Irvine, CA 92697-3875, USA*

(*Received 4 December 2011; final version received 30 August 2012*)

We study scalar waves probing a heterogeneous medium whose parameters are modeled in terms of a statistically isotropic random field. The medium is terminated by an oblique interface at one end (the bottom) and pressure release type boundary conditions at the other end (the top). The tilt of the bottom interface is relatively small so that the dominant contributions to the wave field are confined to a paraxial tube. This study generalizes the basic formulation in terms of Itô–Schrödinger equations in a one-dimensional deterministic background, describing the macrostructure, to one in which the background is more complicated. It provides the first step toward the analysis of scattered waves in general background media modulated by a random microstructure. We discuss in detail the enhanced backscattering phenomenon or weak localization in this setting, with a tilted interface imbedded in the random medium, and find that the backscattering cone does not depend on the tilt. We also find that the enhanced backscattering phenomenon is not affected by the replacement of a specular interface with a diffusive interface.

1. Introduction

We consider scalar waves propagating in a heterogeneous medium. We model the heterogeneities as a realization of a random field with relatively short-scale fluctuations. We characterize the waves that have been reflected off the random medium. The regime we consider here corresponds to beam or long-range propagation. Such a situation is often modeled by paraxial wave equations. In the last decades the paraxial wave equation has emerged as the dominant tool to describe small-scale scattering such as in radio-wave propagation, radar, remote sensing, propagation in urban environments and in underwater acoustics, as well as in propagation problems in the Earth's crust [1,2]. In its basic formulation, this approximation leads to only forward propagating waves, a forward-scattering approximation. Here we consider a generalization that captures also the reflected wave.

*Corresponding author. Email: ksolna@math.uci.edu

ISSN 1745–5030 print/ISSN 1745–5049 online

http://dx.doi.org/10.1080/17455030.2012.728299
http://www.tandfonline.com

In [3] we considered a configuration consisting of a random slab bounded at the bottom by a horizontal interface. We showed that both the paraxial approximation associated with the beam geometry and a white noise approximation associated with the rapid medium fluctuations can be justified simultaneously. For the transmitted field the limit equation takes the form of a random Schrödinger equation studied in particular in [4].

In this paper, we generalize our previous results to the case with a tilted interface at the bottom of the random slab, generating strong reflection, and the presence of a pressure release, or free surface, boundary condition at the top of the slab. The free surface generates multiple reflections, and we derive a characterization of these in terms of a family of reflection operators, the kernels of which satisfy Itô–Schrödinger equations. We discuss in detail how these lead to specific problems for Wigner transforms of the limit kernels which are useful for analyzing the characteristics of the reflected wave field. We use the representation in terms of reflection operators to analyze the spreading and decorrelation of the reflected field.

As a specific application of our result, we consider the enhanced backscattering phenomenon or weak localization effect [5,6]: If a quasi-plane wave is incoming with a given incidence angle, then the mean reflected intensity has a local maximum in the backscattered direction, which is twice as large as the mean reflected intensity in the other directions. This enhancement can be observed in a small cone around the backscattered direction, and it can be interpreted as the result of constructive interferences between reciprocal wave paths. The result we find here is interesting in that in our configuration the backscattering cone depends on the presence of the bottom interface, but does not depend on the tilt. This emphasizes the fact that the enhanced backscattering phenomenon is a coherence effect. This observation is further corroborated by the fact that the structure of the enhanced backscattering cone is not affected by replacing the specular interface by a diffusive interface. We remark that, in this paper, we analyze the partially coherent wave energy being reflected off the interface and the free surface. This situation is different if one considers the wave energy generated by the reflections by the random fluctuations only; such a situation is discussed in [7].

The results obtained in this paper have applications, for example, in reflection seismology. Here, the tilted interface would be a model, locally, of the top of a reservoir, the bottom of the crust or the top of a subducting slab, and one is interested in estimating the location of the interface as well as in characterizing the random fluctuations (“microfabric”) using the (multiple) wave reflections at the top as the data.

The outline of the paper is as follows. We introduce the model and the main separation of scales assumption in Section 2. In Section 3 we carry out the basic wave decomposition in locally up- and down-propagating wave components. This leads to a boundary value formulation and we convert this to an initial value formulation via invariant imbedding in Section 4. We present the main result in Section 5 which shows how we can characterize the wave reflection process and the multiples associated with our formulation via an Itô–Schrödinger equation for the reflection operator. After a brief review of the form of the reflected field in the homogeneous case presented in Section 6, we discuss in detail in Section 7 how the microstructure in our configuration affects the first and second (cross) moments of the

reflected field. We end with a discussion of the enhanced backscattering phenomenon in Section 8.

2. Configuration, scaling and assumptions

We consider acoustic waves propagating in $1+d$ spatial dimensions with random medium fluctuations. The governing equations are

$$\rho(z,\boldsymbol{x})\frac{\partial \boldsymbol{u}}{\partial t}+\nabla p=\boldsymbol{F},\quad \frac{1}{K(z,\boldsymbol{x})}\frac{\partial p}{\partial t}+\nabla\cdot\boldsymbol{u}=0, \tag{1}$$

where p is the pressure field, $\boldsymbol{u}$ is the velocity field, ρ is the density of the medium, K is the bulk modulus of the medium, and $(z,\boldsymbol{x})\in \mathbb{R}\times\mathbb{R}^d$ are the space coordinates. The source is modeled by the forcing term $\boldsymbol{F}$.

We consider in this paper the situation in which a random slab occupies the region

$$\Omega_r=\left\{(z,\boldsymbol{x}),\ \boldsymbol{x}\in\mathbb{R}^{\mathrm{d}},\ z_i(\boldsymbol{x})\le z\le 0\right\}.$$

The surface $z=0$ is the top interface and the surface $z=z_i(\boldsymbol{x})<0$ is the bottom interface. The medium fluctuations in the region Ω_r vary rapidly in space while the "background" medium is constant. The density of the medium is assumed to be evanescent in the region $z>0$, which gives pressure release boundary conditions at the top interface. We consider a mismatch at the boundary $z=z_i(\boldsymbol{x})$, which gives jump conditions at the bottom interface. We denote by ρ_0 and K_0 the background medium parameters in the half-space $z\le z_i(\boldsymbol{x})$, and by ρ_1 and K_1 the parameters in the region Ω_r:

$$\frac{1}{K(z,\boldsymbol{x})}=\begin{cases}K_0^{-1} & \text{if } z\le z_i(\boldsymbol{x}),\\ K_1^{-1}(1+\nu_K(z,\boldsymbol{x})) & \text{if } z\in(z_i(\boldsymbol{x}),0),\\ K_1^{-1} & \text{if } z\ge 0,\end{cases}$$

$$\rho(z,\boldsymbol{x})=\begin{cases}\rho_0 & \text{if } z\le z_i(\boldsymbol{x}),\\ \rho_1 & \text{if } z\in(z_i(\boldsymbol{x}),0),\\ 0 & \text{if } z\ge 0,\end{cases}$$

where the random field $\nu_K(z,\boldsymbol{x})$ models the medium fluctuations, the correlation length of which is l_K.

The source, $\boldsymbol{F}$, is located in the region Ω_r at $z=z_s$, $z_s<0$, close to the surface $z=0$ (we will eventually take the limit $z_s\to 0^-$). We shall refer to waves propagating in the direction with a positive z component as up-going waves. The source generates waves that propagate through the random medium and that are reflected by the interface at $z=z_i(\boldsymbol{x})$ and propagate back through the medium. We are interested in the waves that can be recorded at the surface $z=0$.

The source has the form

$$\boldsymbol{F}(t,z,\boldsymbol{x})=f(t,\boldsymbol{x})\delta(z-z_s)\boldsymbol{e}_z,$$

where $\boldsymbol{e}_z$ is the unit vector pointing in the z-direction. We denote by ω_0 the typical frequency of the source term f and by R_0 the diameter of its spatial support (which

gives the initial beam width). The typical wavelength associated with the typical frequency ω_0 is $\lambda_0 = 2\pi c_1/\omega_0$, for $c_1 = \sqrt{K_1/\rho_1}$ the background speed in the region Ω_r, which is of the same order as the background speed $c_0 = \sqrt{K_0/\rho_0}$ in the half-space $z \leq z_i(\boldsymbol{x})$.

We now introduce the scaling regime that we consider in this paper:

(1) We assume that the correlation length l_K of the medium is much smaller than the typical propagation distance L (of the order of $|z_i|$). We denote by ε^2 the ratio between the correlation length and the typical propagation distance.
(2) We assume that the transverse width of the source R_0 and the correlation length of the medium l_K are of the same order. This means that we assume that the ratio R_0/L is of order ε^2. This scaling is motivated by the fact that, in this regime, there is a non-trivial interaction between the fluctuations of the medium and the beam.
(3) We assume that the typical wavelength λ_0 is much smaller than the propagation distance L; more precisely, we assume that the ratio λ_0/L is of order ε^4. This high-frequency scaling is motivated by the following considerations. The Rayleigh length for a beam with initial width R_0 and central wavelength λ_0 is of the order of R_0^2/λ_0 in the absence of random fluctuations (the Rayleigh length is the distance from the beam waist where the beam area is doubled by diffraction). In order to get a Rayleigh length of the order of the propagation distance L, the ratio λ_0/L must be of order ε^4 since $R_0/L \sim \varepsilon^2$.
(4) We assume that the distance from the surface $z = 0$ to the source $z = z_s$ is of the order of the wavelength (or smaller), that is, of the order of ε^4.
(5) We assume that the bottom interface $z = z_i(\boldsymbol{x})$ is (locally) flat and its normal vector makes a small angle with respect to $\boldsymbol{e}_z$. The magnitude of this angle is of order ε^2, so that Descartes' law predicts that the beam generated by the source and reflected by the interface will be recorded at the surface $z = 0$ with a lateral shift of the order of the radius of the beam. This is the interesting configuration, in which the incident and reflected waves propagate through the same region of the random medium. Furthermore, the pressure release boundary conditions also reflect the waves, so they will experience several round trips between the two interfaces $z = 0$ and $z = z_i(\boldsymbol{x})$.

Henceforth, we shall assume non-dimensionalized units chosen such that the background bulk modulus K_1 and density ρ_1 in the region Ω_r are one; hence, the background speed $c_1 = \sqrt{K_1/\rho_1}$ and impedance $Z_1 = \sqrt{K_1\rho_1}$ are also equal to one. If we consider the propagation distance, L, as our reference distance of order one in this scaled regime, then

(1) the equation of the bottom interface is $z = -L - \varepsilon^2\boldsymbol{\theta}\cdot\boldsymbol{x}$ where $\boldsymbol{\theta} \in \mathbb{R}^d$ with $|\boldsymbol{\theta}| = 1$ and $L > 0$ is the depth of the interface;
(2) the source is localized at $z = -\varepsilon^4 z_0$ and it has the form

$$\boldsymbol{F}(t, z, \boldsymbol{x}) = f\Big(\frac{t}{\varepsilon^4}, \frac{\boldsymbol{x}}{\varepsilon^2}\Big)\delta\big(z + \varepsilon^4 z_0\big)\boldsymbol{e}_z, \tag{2}$$

where $z_0 > 0$ and $f(t, \boldsymbol{x})$ is the normalized source shape function (with time and spatial scales of variations of order one);

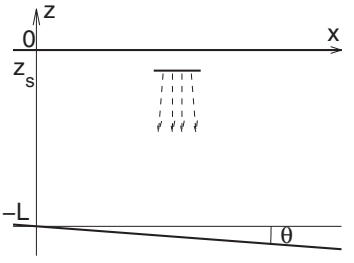

Figure 1. Configuration: The source is located at depth $z_s < 0$ close to the surface. An oblique interface is specified by $(-L, 0)$ and θ.

(3) the medium fluctuations have the form

$$\frac{1}{K(z,\boldsymbol{x})} = \begin{cases} K_0^{-1} & \text{if } z \le -L - \varepsilon^2 \boldsymbol{\theta}\cdot\boldsymbol{x}, \\ 1 + \varepsilon^3 \nu\Big(\dfrac{z}{\varepsilon^2}, \dfrac{\boldsymbol{x}}{\varepsilon^2}\Big) & \text{if } z \in (-L - \varepsilon^2\boldsymbol{\theta}\cdot\boldsymbol{x}, 0), \\ 1 & \text{if } z \ge 0, \end{cases}$$

$$\rho(z,\boldsymbol{x}) = \begin{cases} \rho_0 & \text{if } z \le -L - \varepsilon^2 \boldsymbol{\theta}\cdot\boldsymbol{x}, \\ 1 & \text{if } z \in (-L - \varepsilon^2\boldsymbol{\theta}\cdot\boldsymbol{x}, 0), \\ 0 & \text{if } z \ge 0, \end{cases}$$

where the zero-mean, stationary random field ν has a correlation length of order one and standard deviation of order one, see Figure 1. We also assume that it satisfies strong mixing conditions in z. Here the amplitude ε^3 of the fluctuations has been chosen so as to obtain an effective regime of order one when ε goes to zero. That is, if the magnitude of the fluctuations is smaller than ε^3, then the wave would propagate as if the medium were homogeneous, while if the order of magnitude is larger, then the wave would not penetrate the slab down to the bottom interface. The scaling that we consider here corresponds to the physically most interesting situation.

3. The boundary value problem

Since both the medium and the source have transverse spatial variations at the scale ε^2, it is convenient to rescale the transverse coordinates $\boldsymbol{x}/\varepsilon^2 \to \boldsymbol{x}$ and to introduce the rescaled fields $\boldsymbol{u}^\varepsilon$ and p^ε:

$$\boldsymbol{u}^\varepsilon(t,z,\boldsymbol{x}) = \boldsymbol{u}(t, z - \varepsilon^4\boldsymbol{\theta}\cdot\boldsymbol{x}, \varepsilon^2\boldsymbol{x}), \quad p^\varepsilon(t,z,\boldsymbol{x}) = p(t, z - \varepsilon^4\boldsymbol{\theta}\cdot\boldsymbol{x}, \varepsilon^2\boldsymbol{x}). \tag{3}$$

In these new coordinates, the bottom interface is $z = -L$ while the top surface is $z = \varepsilon^4\boldsymbol{\theta}\cdot\boldsymbol{x}$. This transformation is convenient for the invariant imbedding formulation that we present below. In the region Ω_r the fields satisfy

$$\frac{\partial \boldsymbol{u}^\varepsilon}{\partial t} + \begin{bmatrix} \partial_z \\ \varepsilon^2\boldsymbol{\theta}\partial_z + \varepsilon^{-2}\nabla_{\boldsymbol{x}} \end{bmatrix} p^\varepsilon = f\Big(\frac{t}{\varepsilon^4}, \boldsymbol{x}\Big)\delta\big(z + \varepsilon^4(z_0 - \boldsymbol{\theta}\cdot\boldsymbol{x})\big)\begin{bmatrix} 1 \\ \mathbf{0} \end{bmatrix}, \tag{4}$$

$$\Big(1 + \varepsilon^3\nu\Big(\frac{z}{\varepsilon^2} - \varepsilon^2\boldsymbol{\theta}\cdot\boldsymbol{x}, \boldsymbol{x}\Big)\Big)\frac{\partial p^\varepsilon}{\partial t} + \begin{bmatrix} \partial_z \\ \varepsilon^2\boldsymbol{\theta}\partial_z + \varepsilon^{-2}\nabla_{\boldsymbol{x}} \end{bmatrix} \cdot \boldsymbol{u}^\varepsilon = 0, \tag{5}$$

where $\nabla_{\boldsymbol{x}}$ stands for the gradient with respect to the transverse spatial variables $\boldsymbol{x}$. The pressure field and its z-derivative in the region Ω_r can be written as:

$$p^\varepsilon(t,z,\boldsymbol{x}) = \frac{1}{2\pi}\int \Big(\widetilde{a}^\varepsilon(k,z,\boldsymbol{x})e^{ik\frac{z}{\varepsilon^4}} + \widetilde{b}^\varepsilon(k,z,\boldsymbol{x})e^{-ik\frac{z}{\varepsilon^4}}\Big)e^{-ik\frac{t}{\varepsilon^4}}\,\mathrm{d}k,$$
$$\frac{\partial p^\varepsilon}{\partial z}(t,z,\boldsymbol{x}) = \frac{1}{2\pi}\int \frac{ik}{\varepsilon^4}\Big(\widetilde{a}^\varepsilon(k,z,\boldsymbol{x})e^{ik\frac{z}{\varepsilon^4}} - \widetilde{b}^\varepsilon(k,z,\boldsymbol{x})e^{-ik\frac{z}{\varepsilon^4}}\Big)e^{-ik\frac{t}{\varepsilon^4}}\,\mathrm{d}k,$$

with the complex amplitudes $\widetilde{a}^\varepsilon$ and $\widetilde{b}^\varepsilon$ of the up- and down-propagating modes given explicitly by

$$\widetilde{a}^\varepsilon(k,z,\boldsymbol{x}) = \frac{1}{2}\left[\int\left(\frac{1}{\varepsilon^4}p^\varepsilon(t,z,\boldsymbol{x}) + \frac{1}{ik}\frac{\partial p^\varepsilon}{\partial z}(t,z,\boldsymbol{x})\right)e^{ik\frac{t}{\varepsilon^4}}\,\mathrm{d}t\right]e^{-ik\frac{z}{\varepsilon^4}},$$
$$\widetilde{b}^\varepsilon(k,z,\boldsymbol{x}) = \frac{1}{2}\left[\int\left(\frac{1}{\varepsilon^4}p^\varepsilon(t,z,\boldsymbol{x}) - \frac{1}{ik}\frac{\partial p^\varepsilon}{\partial z}(t,z,\boldsymbol{x})\right)e^{ik\frac{t}{\varepsilon^4}}\,\mathrm{d}t\right]e^{ik\frac{z}{\varepsilon^4}}.$$

The pressure release boundary conditions impose $p^\varepsilon(t,\, z=\varepsilon^4\boldsymbol{\theta}\cdot\boldsymbol{x},\boldsymbol{x}) = 0$.

Using (4)–(5) we obtain after Fourier transform, elimination of $\boldsymbol{u}^\varepsilon$, and the use of the above definitions of $\widetilde{a}^\varepsilon, \widetilde{b}^\varepsilon$, that the mode amplitudes satisfy the coupled equations

$$\frac{\partial\widetilde{a}^\varepsilon}{\partial z} = \left(\frac{ik}{2\varepsilon}\nu\Big(\frac{z}{\varepsilon^2},\boldsymbol{x}\Big) + \frac{i}{2k}\Delta_{\boldsymbol{x}}\right)\widetilde{a}^\varepsilon + e^{-2ik\frac{z}{\varepsilon^4}}\left(\frac{ik}{2\varepsilon}\nu\Big(\frac{z}{\varepsilon^2},\boldsymbol{x}\Big) + \frac{i}{2k}\Delta_{\boldsymbol{x}}\right)\widetilde{b}^\varepsilon, \tag{6}$$

$$\frac{\partial\widetilde{b}^\varepsilon}{\partial z} = -e^{2ik\frac{z}{\varepsilon^4}}\left(\frac{ik}{2\varepsilon}\nu\Big(\frac{z}{\varepsilon^2},\boldsymbol{x}\Big) + \frac{i}{2k}\Delta_{\boldsymbol{x}}\right)\widetilde{a}^\varepsilon - \left(\frac{ik}{2\varepsilon}\nu\Big(\frac{z}{\varepsilon^2},\boldsymbol{x}\Big) + \frac{i}{2k}\Delta_{\boldsymbol{x}}\right)\widetilde{b}^\varepsilon, \tag{7}$$

where we have neglected terms of order ε^2. Note that the z-derivatives of $\widetilde{a}^\varepsilon$ and $\widetilde{b}^\varepsilon$ are of the order of ε^{-1}, so we have to leading order $\widetilde{a}^\varepsilon(k,z,\boldsymbol{x}) = \widetilde{a}^\varepsilon(k,0^+,\boldsymbol{x})$ and $\widetilde{b}^\varepsilon(k,z,\boldsymbol{x}) = \widetilde{b}^\varepsilon(k,0^+,\boldsymbol{x})$ for $z\in(-\varepsilon^4 z_0+\varepsilon^4\boldsymbol{\theta}\cdot\boldsymbol{x},\, \varepsilon^4\boldsymbol{\theta}\cdot\boldsymbol{x})$ (the region between the source and the top surface), and we denote by $\widetilde{a}^\varepsilon(k,0^-,\boldsymbol{x})$ and $\widetilde{b}^\varepsilon(k,0^-,\boldsymbol{x})$ the values of $\widetilde{a}^\varepsilon(k,z,\boldsymbol{x})$ and $\widetilde{b}^\varepsilon(k,z,\boldsymbol{x})$ just below the source.

The system (6)–(7) is valid in $z\in(-L,0)$ and it is complemented with the following boundary and jump conditions at $z=0^+$ (the top interface), $z=0^-$ (the source) and $z=-L$ (the bottom interface):

$$\widetilde{a}^\varepsilon(k,0^+,\boldsymbol{x})e^{ik\boldsymbol{\theta}\cdot\boldsymbol{x}} + \widetilde{b}^\varepsilon(k,0^+,\boldsymbol{x})e^{-ik\boldsymbol{\theta}\cdot\boldsymbol{x}} = 0, \tag{8}$$

$$\Big[\widetilde{a}^\varepsilon(k,0^+,\boldsymbol{x})e^{-ik(z_0-\boldsymbol{\theta}\cdot\boldsymbol{x})} + \widetilde{b}^\varepsilon(k,0^+,\boldsymbol{x})e^{ik(z_0-\boldsymbol{\theta}\cdot\boldsymbol{x})}\Big] - \Big[\widetilde{a}^\varepsilon(k,0^-,\boldsymbol{x})e^{-ik(z_0-\boldsymbol{\theta}\cdot\boldsymbol{x})} + \widetilde{b}^\varepsilon(k,0^-,\boldsymbol{x})e^{ik(z_0-\boldsymbol{\theta}\cdot\boldsymbol{x})}\Big] = \widetilde{f}(k,\boldsymbol{x}), \tag{9}$$

$$\Big[\widetilde{a}^\varepsilon(k,0^+,\boldsymbol{x})e^{-ik(z_0-\boldsymbol{\theta}\cdot\boldsymbol{x})} - \widetilde{b}^\varepsilon(k,0^+,\boldsymbol{x})e^{ik(z_0-\boldsymbol{\theta}\cdot\boldsymbol{x})}\Big] - \Big[\widetilde{a}^\varepsilon(k,0^-,\boldsymbol{x})e^{-ik(z_0-\boldsymbol{\theta}\cdot\boldsymbol{x})} - \widetilde{b}^\varepsilon(k,0^-,\boldsymbol{x})e^{ik(z_0-\boldsymbol{\theta}\cdot\boldsymbol{x})}\Big] = 0, \tag{10}$$

$$\widetilde{a}^\varepsilon(k,-L,\boldsymbol{x})e^{-ik\frac{L}{\varepsilon^4}} - \mathcal{R}_0\widetilde{b}^\varepsilon(k,-L,\boldsymbol{x})e^{ik\frac{L}{\varepsilon^4}} = 0, \tag{11}$$

where $\mathcal{R}_0=(Z_0-1)/(Z_0+1)$ is the reflection coefficient of the bottom interface, $Z_0=\sqrt{K_0\rho_0}$ is the impedance of the bottom homogeneous half-space, and the Fourier transforms are defined by

$$\widetilde{f}(k,\boldsymbol{x})=\int f(t,\boldsymbol{x})e^{ikt}\,\mathrm{d}t,\quad \hat{f}(k,\boldsymbol{\kappa})=\int \widetilde{f}(k,\boldsymbol{x})e^{-i\boldsymbol{\kappa}\cdot\boldsymbol{x}}\,\mathrm{d}\boldsymbol{x}. \tag{12}$$

We simplify condition (9) by taking $z_0\to 0$ (which means that the distance from the source to the top interface is smaller than the wavelength), and we find that the system (6)–(7) in $z\in(-L,0)$ is complemented with boundary conditions (11) at $z=-L$ and

$$\widetilde{b}^\varepsilon(k,0^-,\boldsymbol{x})+\widetilde{a}^\varepsilon(k,0^-,\boldsymbol{x})e^{2ik\boldsymbol{\theta}\cdot\boldsymbol{x}}=-\widetilde{f}(k,\boldsymbol{x})e^{ik\boldsymbol{\theta}\cdot\boldsymbol{x}}, \tag{13}$$

at $z=0^-$. The waves that can be observed at the surface $z=0^+$ are given by

$$\widetilde{a}^\varepsilon(k,0^+,\boldsymbol{x})=\frac{1}{2}\widetilde{a}^\varepsilon(k,0^-,\boldsymbol{x})-\frac{1}{2}\widetilde{b}^\varepsilon(k,0^-,\boldsymbol{x})e^{-2ik\boldsymbol{\theta}\cdot\boldsymbol{x}}, \tag{14}$$

$$\widetilde{b}^\varepsilon(k,0^+,\boldsymbol{x})=-\frac{1}{2}\widetilde{a}^\varepsilon(k,0^-,\boldsymbol{x})e^{2ik\boldsymbol{\theta}\cdot\boldsymbol{x}}+\frac{1}{2}\widetilde{b}^\varepsilon(k,0^-,\boldsymbol{x}). \tag{15}$$

The signals recorded at the surface are in practice the vertical velocity (normal to the top surface) defined by

$$v^\varepsilon(t,\boldsymbol{x}):=\boldsymbol{e}_z\cdot\boldsymbol{u}(t,0,\varepsilon^2\boldsymbol{x}), \tag{16}$$

which is such that

$$\frac{\partial v^\varepsilon}{\partial t}(t,\boldsymbol{x})=-\frac{\partial p^\varepsilon}{\partial z}(t,\varepsilon^4\boldsymbol{\theta}\cdot\boldsymbol{x},\boldsymbol{x}).$$

Therefore

$$v^\varepsilon(t,\boldsymbol{x})=\frac{1}{2\pi}\int\Big(\widetilde{a}^\varepsilon(k,0^+,\boldsymbol{x})e^{ik\boldsymbol{\theta}\cdot\boldsymbol{x}}-\widetilde{b}^\varepsilon(k,0^+,\boldsymbol{x})e^{-ik\boldsymbol{\theta}\cdot\boldsymbol{x}}\Big)e^{-ik\frac{t}{\varepsilon^4}}\,\mathrm{d}k. \tag{17}$$

4. The reflection operator

We define the lateral Fourier modes

$$\hat{a}^\varepsilon(k,z,\boldsymbol{\kappa})=\int\widetilde{a}^\varepsilon(k,z,\boldsymbol{x})e^{-i\boldsymbol{\kappa}\cdot\boldsymbol{x}}\,\mathrm{d}\boldsymbol{x},\quad \hat{b}^\varepsilon(k,z,\boldsymbol{\kappa})=\int\widetilde{b}^\varepsilon(k,z,\boldsymbol{x})e^{-i\boldsymbol{\kappa}\cdot\boldsymbol{x}}\,\mathrm{d}\boldsymbol{x}. \tag{18}$$

They satisfy for $z\in(-L,0)$

$$\frac{\mathrm{d}\hat{a}^\varepsilon}{\mathrm{d}z}(k,z,\boldsymbol{\kappa})=\int\widehat{\boldsymbol{\mathcal{L}}}^\varepsilon(k,z,\boldsymbol{\kappa},\boldsymbol{\kappa}')\hat{a}^\varepsilon(k,z,\boldsymbol{\kappa}')\mathrm{d}\boldsymbol{\kappa}'+e^{-\frac{2ikz}{\varepsilon^4}}\int\widehat{\boldsymbol{\mathcal{L}}}^\varepsilon(k,z,\boldsymbol{\kappa},\boldsymbol{\kappa}')\hat{b}^\varepsilon(k,z,\boldsymbol{\kappa}')\mathrm{d}\boldsymbol{\kappa}',$$

$$\frac{\mathrm{d}\hat{b}^\varepsilon}{\mathrm{d}z}(k,z,\boldsymbol{\kappa})=-e^{-\frac{2ikz}{\varepsilon^4}}\int\widehat{\boldsymbol{\mathcal{L}}}^\varepsilon(k,z,\boldsymbol{\kappa},\boldsymbol{\kappa}')\hat{a}^\varepsilon(k,z,\boldsymbol{\kappa}')\mathrm{d}\boldsymbol{\kappa}'-\int\widehat{\boldsymbol{\mathcal{L}}}^\varepsilon(k,z,\boldsymbol{\kappa},\boldsymbol{\kappa}')\hat{b}^\varepsilon(k,z,\boldsymbol{\kappa}')\mathrm{d}\boldsymbol{\kappa}',$$

where

$$\widehat{\mathcal{L}}^{\varepsilon}(k,z,\boldsymbol{\kappa}_1,\boldsymbol{\kappa}_2)=-\frac{i}{2k}|\boldsymbol{\kappa}_1|^2\delta(\boldsymbol{\kappa}_1-\boldsymbol{\kappa}_2)+\frac{ik}{2(2\pi)^d\varepsilon}\hat{\nu}\Big(\frac{z}{\varepsilon^2},\boldsymbol{\kappa}_1-\boldsymbol{\kappa}_2\Big), \tag{19}$$

with $\hat{\boldsymbol{\nu}}(z,\boldsymbol{\kappa})$ the partial Fourier transform (in x) of $\nu(z,\boldsymbol{x})$. The boundary conditions (11) and (13) at $z=-L$ and $z=0^-$ read

$$\hat{a}^{\varepsilon}(k,-L,\boldsymbol{\kappa})e^{-ik\frac{L}{\varepsilon^4}}-\mathcal{R}_0\hat{b}^{\varepsilon}(k,-L,\boldsymbol{\kappa})e^{ik\frac{L}{\varepsilon^4}}=0, \tag{20}$$

$$\hat{b}^{\varepsilon}(k,0^-,\boldsymbol{\kappa})+\hat{a}^{\varepsilon}(k,0^-,\boldsymbol{\kappa}-2k\boldsymbol{\theta})=-\hat{f}(k,\boldsymbol{\kappa}-k\boldsymbol{\theta}). \tag{21}$$

We now apply an invariant imbedding technique to obtain that

$$\hat{b}^{\varepsilon}(k,-L,\boldsymbol{\kappa})=\int\widehat{\mathcal{T}}^{\varepsilon}(k,z,\boldsymbol{\kappa},\boldsymbol{\kappa}')\hat{b}^{\varepsilon}(k,z,\boldsymbol{\kappa}')\mathrm{d}\boldsymbol{\kappa}', \tag{22}$$

$$\hat{a}^{\varepsilon}(k,z,\boldsymbol{\kappa})=e^{2ik\frac{L}{\varepsilon^4}}\int\widehat{\mathcal{R}}^{\varepsilon}(k,z,\boldsymbol{\kappa},\boldsymbol{\kappa}')\hat{b}^{\varepsilon}(k,z,\boldsymbol{\kappa}')\mathrm{d}\boldsymbol{\kappa}', \tag{23}$$

where the kernels of the operators $\widehat{\mathcal{T}}^{\varepsilon}$ and $\widehat{\mathcal{R}}^{\varepsilon}$ satisfy

$$\begin{aligned}\frac{\mathrm{d}}{\mathrm{d}z}\widehat{\mathcal{R}}^{\varepsilon}(k,z,\boldsymbol{\kappa},\boldsymbol{\kappa}')&=e^{-\frac{2ik(z+L)}{\varepsilon^4}}\widehat{\mathcal{L}}^{\varepsilon}(k,z,\boldsymbol{\kappa},\boldsymbol{\kappa}')+\int\widehat{\mathcal{L}}^{\varepsilon}(k,z,\boldsymbol{\kappa},\boldsymbol{\kappa}_1)\widehat{\mathcal{R}}^{\varepsilon}(k,z,\boldsymbol{\kappa}_1,\boldsymbol{\kappa}')\mathrm{d}\boldsymbol{\kappa}_1\\&\quad+\int\widehat{\mathcal{R}}^{\varepsilon}(k,z,\boldsymbol{\kappa},\boldsymbol{\kappa}_1)\widehat{\mathcal{L}}^{\varepsilon}(k,z,\boldsymbol{\kappa}_1,\boldsymbol{\kappa}')\mathrm{d}\boldsymbol{\kappa}_1+e^{\frac{2ik(z+L)}{\varepsilon^4}}\int\int\widehat{\mathcal{R}}^{\varepsilon}(k,z,\boldsymbol{\kappa},\boldsymbol{\kappa}_1)\\&\quad\times\widehat{\mathcal{L}}^{\varepsilon}(k,z,\boldsymbol{\kappa}_1,\boldsymbol{\kappa}_2)\widehat{\mathcal{R}}^{\varepsilon}(k,z,\boldsymbol{\kappa}_2,\boldsymbol{\kappa}')\,\mathrm{d}\boldsymbol{\kappa}_1\mathrm{d}\boldsymbol{\kappa}_2,\end{aligned} \tag{24}$$

$$\begin{aligned}\frac{\mathrm{d}}{\mathrm{d}z}\widehat{\mathcal{T}}^{\varepsilon}(k,z,\boldsymbol{\kappa},\boldsymbol{\kappa}')&=\int\widehat{\mathcal{T}}^{\varepsilon}(k,z,\boldsymbol{\kappa},\boldsymbol{\kappa}_1)\widehat{\mathcal{L}}^{\varepsilon}(k,z,\boldsymbol{\kappa}_1,\boldsymbol{\kappa}')\mathrm{d}\boldsymbol{\kappa}_1+e^{\frac{2ik(z+L)}{\varepsilon^4}}\int\int\widehat{\mathcal{T}}^{\varepsilon}(k,z,\boldsymbol{\kappa},\boldsymbol{\kappa}_1)\\&\quad\times\widehat{\mathcal{L}}^{\varepsilon}(k,z,\boldsymbol{\kappa}_1,\boldsymbol{\kappa}_2)\widehat{\mathcal{R}}^{\varepsilon}(k,z,\boldsymbol{\kappa}_2,\boldsymbol{\kappa}')\,\mathrm{d}\boldsymbol{\kappa}_1\mathrm{d}\boldsymbol{\kappa}_2.\end{aligned} \tag{25}$$

This system is complemented with the initial conditions at $z=-L$, which are obtained from (20):

$$\widehat{\mathcal{R}}^{\varepsilon}(k,-L,\boldsymbol{\kappa},\boldsymbol{\kappa}')=\mathcal{R}_0\delta(\boldsymbol{\kappa}-\boldsymbol{\kappa}'),\quad\widehat{\mathcal{T}}^{\varepsilon}(k,-L,\boldsymbol{\kappa},\boldsymbol{\kappa}')=\delta(\boldsymbol{\kappa}-\boldsymbol{\kappa}').$$

The transmission and reflection operators evaluated at $z=0^-$ carry all the relevant information about the random medium from the point of view of the transmitted and reflected waves.

Using (21) and (23) we find

$$\hat{b}^{\varepsilon}(k,0^-,\boldsymbol{\kappa})=-\hat{f}(k,\boldsymbol{\kappa}-k\boldsymbol{\theta})-e^{2ik\frac{L}{\varepsilon^4}}\int\widehat{\mathcal{R}}^{\varepsilon}(k,0,\boldsymbol{\kappa}-2k\boldsymbol{\theta},\boldsymbol{\kappa}')\hat{b}^{\varepsilon}(k,0^-,\boldsymbol{\kappa}')\mathrm{d}\boldsymbol{\kappa}'.$$

The solution of this equation can be expanded as a series:

$$\begin{aligned}\hat{b}^{\varepsilon}(k,0^-,\boldsymbol{\kappa})&=-\hat{f}(k,\boldsymbol{\kappa}-k\boldsymbol{\theta})+e^{2ik\frac{L}{\varepsilon^4}}\int\widehat{\mathcal{R}}^{\varepsilon}(k,0,\boldsymbol{\kappa}-2k\boldsymbol{\theta},\boldsymbol{\kappa}_1+k\boldsymbol{\theta})\hat{f}(k,\boldsymbol{\kappa}_1)\mathrm{d}\boldsymbol{\kappa}_1\\&\quad-e^{4ik\frac{L}{\varepsilon^4}}\int\int\widehat{\mathcal{R}}^{\varepsilon}(k,0,\boldsymbol{\kappa}-2k\boldsymbol{\theta},\boldsymbol{\kappa}_1+k\boldsymbol{\theta})\end{aligned}$$

$$\times \widehat{\mathcal{R}}^{\varepsilon}(k,0,\boldsymbol{\kappa}_1 - k\boldsymbol{\theta}, \boldsymbol{\kappa}_2 + k\boldsymbol{\theta})\hat{f}(k,\boldsymbol{\kappa}_2)\mathrm{d}\boldsymbol{\kappa}_1\mathrm{d}\boldsymbol{\kappa}_2$$
$$+ e^{6ik\frac{L}{\varepsilon^4}}\cdots,$$
$$\hat{a}^{\varepsilon}(k,0^-,\boldsymbol{\kappa}) = -\hat{f}(k,\boldsymbol{\kappa}+k\boldsymbol{\theta}) - \hat{b}^{\varepsilon}(k,0^-,\boldsymbol{\kappa}+2k\boldsymbol{\theta}),$$

and therefore

$$\hat{b}^{\varepsilon}(k,0^+,\boldsymbol{\kappa}) = \hat{b}^{\varepsilon}(k,0^-,\boldsymbol{\kappa}) + \frac{1}{2}\hat{f}(k,\boldsymbol{\kappa}-k\boldsymbol{\theta}),$$
$$\hat{a}^{\varepsilon}(k,0^+,\boldsymbol{\kappa}) = \hat{a}^{\varepsilon}(k,0^-,\boldsymbol{\kappa}) + \frac{1}{2}\hat{f}(k,\boldsymbol{\kappa}+k\boldsymbol{\theta}),$$
$$\hat{a}^{\varepsilon}(k,0^+,\boldsymbol{\kappa}-k\boldsymbol{\theta}) - \hat{b}^{\varepsilon}(k,0^+,\boldsymbol{\kappa}+k\boldsymbol{\theta})$$
$$= \hat{f}(k,\boldsymbol{\kappa}) - e^{2ik\frac{L}{\varepsilon^4}}\int \widehat{\mathcal{R}}^{\varepsilon}(k,0,\boldsymbol{\kappa}-k\boldsymbol{\theta},\boldsymbol{\kappa}_1+k\boldsymbol{\theta})\hat{f}(k,\boldsymbol{\kappa}_1)\mathrm{d}\boldsymbol{\kappa}_1$$
$$+ e^{4ik\frac{L}{\varepsilon^4}}\int\int \widehat{\mathcal{R}}^{\varepsilon}(k,0,\boldsymbol{\kappa}-k\boldsymbol{\theta},\boldsymbol{\kappa}_1+k\boldsymbol{\theta})$$
$$\times \widehat{\mathcal{R}}^{\varepsilon}(k,0,\boldsymbol{\kappa}_1-k\boldsymbol{\theta},\boldsymbol{\kappa}_2+k\boldsymbol{\theta})\hat{f}(k,\boldsymbol{\kappa}_2)\mathrm{d}\boldsymbol{\kappa}_1\mathrm{d}\boldsymbol{\kappa}_2$$
$$+ e^{6ik\frac{L}{\varepsilon^4}}\cdots. \tag{26}$$

It is straightforward to establish the convergence of the series in the absence of a random field. In the presence of random fluctuations the convergence requires that $\hat{\nu}(z,\boldsymbol{\kappa})$ decays sufficiently fast in $|\boldsymbol{\kappa}|$.

Our objective is to characterize the reflected vertical velocity field (17) around the sequence of expected arrival times $2jL$ (which is j times the round trip time from the surface to the bottom interface):

$$v_j^{\varepsilon}(s,\boldsymbol{x}) := v^{\varepsilon}(2jL+\varepsilon^4 s,\boldsymbol{x})$$
$$= \frac{1}{(2\pi)^{d+1}}\int\int\left[\hat{a}^{\varepsilon}(k,0^+,\boldsymbol{\kappa}-k\boldsymbol{\theta}) - \hat{b}^{\varepsilon}(k,0^+,\boldsymbol{\kappa}+k\boldsymbol{\theta})\right]$$
$$\times e^{i(\boldsymbol{\kappa}\cdot\boldsymbol{x}-ks)}e^{-2ijk\frac{L}{\varepsilon^4}}\mathrm{d}\boldsymbol{\kappa}\,\mathrm{d}k. \tag{27}$$

The presence of the rapid phase factor in (27) selects the term with the opposite rapid phase in the sum (26) in the limit $\varepsilon \to 0$. The kernel of the reflection operator in spatial coordinates is given by

$$\widetilde{\mathcal{R}}^{\varepsilon}(k,z,\boldsymbol{x},\boldsymbol{x}') = \frac{1}{(2\pi)^d}\int\int e^{i(\boldsymbol{x}\cdot\boldsymbol{\kappa}-\boldsymbol{x}'\cdot\boldsymbol{\kappa}')}\widehat{\mathcal{R}}^{\varepsilon}(k,z,\boldsymbol{\kappa},\boldsymbol{\kappa}')\mathrm{d}\boldsymbol{\kappa}\,\mathrm{d}\boldsymbol{\kappa}'. \tag{28}$$

In the next section, we will discuss an "effective" scaling limit representation of this, in the sense that it is a representation that gives the correct statistics for the reflected wave field.

5. The asymptotic representation of the reflected field

We consider the reflected fields v_j^{ε} defined by (27) and use diffusion approximation theorems to identify a limit random Schrödinger model. The main result is the following one.

Proposition 5.1 *For all j, the processes $(v_j^\varepsilon(s,\boldsymbol{x}))_{s\in\mathbb{R},\,\boldsymbol{x}\in\mathbb{R}^d}$ converge in distribution as $\varepsilon\to 0$ in the space $C^0(\mathbb{R},\,L^2(\mathbb{R}^d,\mathbb{R}))\cap L^2(\mathbb{R},\,L^2(\mathbb{R}^d,\mathbb{R}))$ to the limit process $(v_j(s,\boldsymbol{x}))_{s\in\mathbb{R},\,\boldsymbol{x}\in\mathbb{R}^d}$. We have in particular*

$$v_0(s,\boldsymbol{x})=\frac{1}{2\pi}\int\widetilde{f}(k,\boldsymbol{x})e^{-iks}\,\mathrm{d}k, \tag{29}$$

$$v_1(s,\boldsymbol{x})=-\frac{1}{2\pi}\int\int\widetilde{\boldsymbol{\mathcal{R}}}(k,0,\boldsymbol{x},\boldsymbol{x}')e^{ik\boldsymbol{\theta}\cdot\boldsymbol{x}+ik\boldsymbol{\theta}\cdot\boldsymbol{x}'}\widetilde{f}(k,\boldsymbol{x}')\mathrm{d}\boldsymbol{x}'e^{-iks}\,\mathrm{d}k, \tag{30}$$

$$v_2(s,\boldsymbol{x})=\frac{1}{2\pi}\int\int\int\widetilde{\boldsymbol{\mathcal{R}}}(k,0,\boldsymbol{x},\boldsymbol{x}')\widetilde{\boldsymbol{\mathcal{R}}}(k,0,\boldsymbol{x}',\boldsymbol{x}'')e^{ik\boldsymbol{\theta}\cdot\boldsymbol{x}+2ik\boldsymbol{\theta}\cdot\boldsymbol{x}'+ik\boldsymbol{\theta}\cdot\boldsymbol{x}''}\widetilde{f}(k,\boldsymbol{x}'')\mathrm{d}\boldsymbol{x}'\,\mathrm{d}\boldsymbol{x}''e^{-iks}\,\mathrm{d}k. \tag{31}$$

Here $C^0(\mathbb{R},L^2(\mathbb{R}^d,\mathbb{R}))$ is the space of continuous functions (in s) with values in $L^2(\mathbb{R}^d,\mathbb{R})$ and $L^2(\mathbb{R},L^2(\mathbb{R}^d,\mathbb{R}))=L^2(\mathbb{R}\times\mathbb{R}^d,\mathbb{R})$. The kernel of the operator $\widetilde{\boldsymbol{\mathcal{R}}}(k,z,\boldsymbol{x},\boldsymbol{x}')$ is the solution of the following Itô–Schrödinger model

$$\mathrm{d}\widetilde{\boldsymbol{\mathcal{R}}}(k,z,\boldsymbol{x},\boldsymbol{x}')=\frac{i}{2k}(\Delta_{\boldsymbol{x}}+\Delta_{\boldsymbol{x}'})\widetilde{\boldsymbol{\mathcal{R}}}(k,z,\boldsymbol{x},\boldsymbol{x}')\mathrm{d}z+\frac{ik}{2}\widetilde{\boldsymbol{\mathcal{R}}}(k,z,\boldsymbol{x},\boldsymbol{x}')\circ(dB(z,\boldsymbol{x})+dB(z,\boldsymbol{x}')), \tag{32}$$

with the initial condition at $z=-L$:

$$\widetilde{\boldsymbol{\mathcal{R}}}(k,\,-L,\boldsymbol{x},\boldsymbol{x}')=\mathcal{R}_0\delta(\boldsymbol{x}-\boldsymbol{x}').$$

The symbol $\circ$ stands for the Stratonovich stochastic integral, $B(z,\boldsymbol{x})$ is a real-valued Brownian field with covariance

$$\mathbb{E}[B(z_1,\boldsymbol{x}_1)B(z_2,\boldsymbol{x}_2)]=\min\{z_1,z_2\}D(\boldsymbol{x}_1-\boldsymbol{x}_2), \tag{33}$$

and we have used the notations

$$C(z,\boldsymbol{x})=\mathbb{E}[\nu(z'+z,\boldsymbol{x}'+\boldsymbol{x})\nu(z',\boldsymbol{x}')], \tag{34}$$

$$D(\boldsymbol{x})=\int_{-\infty}^{\infty}C(z,\boldsymbol{x})\mathrm{d}z. \tag{35}$$

The moments of the finite-dimensional distributions also converge, in the sense that

$$\mathbb{E}\left[\prod_{l=1}^{q}v_j^\varepsilon(s_l,\boldsymbol{x}_l)^{m_l}\right]\xrightarrow{\varepsilon\to 0}\mathbb{E}\left[\prod_{l=1}^{q}v_j(s_l,\boldsymbol{x}_l)^{m_l}\right], \tag{36}$$

for any $q\in\mathbb{N}$, $(s_l)_{l=1,\ldots,q}\in\mathbb{R}^q$, $(\boldsymbol{x}_l)_{l=1,\ldots,q}\in\mathbb{R}^{dq}$, and $(m_l)_{l=1,\ldots,q}\in\mathbb{N}^q$.

The convergence of the reflected kernel was studied in [3] in the scaling regime outlined in Section 2. As mentioned before we assume that the random process ν has mixing properties in z which ensures that the integrated covariance D in (35) is finite. Moreover

$$v_0(s,\boldsymbol{x})=f(s,\boldsymbol{x})$$

is the field directly emitted upward by the source to the surface, while $v_1(s,\boldsymbol{x})$ is the field emitted downward by the source and that has been reflected once by the

bottom interface. The fields $v_j, j \geq 2$, are the multiples that have been reflected j times by the bottom interface and by the top surface. The statistical properties of the operator $\widetilde{\boldsymbol{\mathcal{R}}}$ have been studied in [3]. Therefore we can use the results contained in that paper in order to analyze the statistical properties of the recorded vertical velocity field.

6. Absence of random fluctuations – Explicit representations

If the medium is homogeneous, then

$$\widetilde{\boldsymbol{\mathcal{R}}}(k,0,\boldsymbol{x},\boldsymbol{x}') = \mathcal{R}_0\left(\frac{k}{4\pi L}\right)^{d/2} e^{-i\frac{\pi d}{4}} \exp\left(-i\frac{k|\boldsymbol{x}-\boldsymbol{x}'|^2}{4L}\right).$$

Let us assume that the source has the form

$$f(t,\boldsymbol{x}) = f_0(t)e^{-ik_0 t}\exp\left(-\frac{|\boldsymbol{x}|^2}{2r_0^2}\right),$$

and that the bandwidth of $f_0(t)$ is smaller than the carrier frequency k_0. Then

$$|v_1(t,\boldsymbol{x})|^2 = \mathcal{R}_0^2\left(1+\frac{4L^2}{k_0^2 r_0^4}\right)^{-d}|f_0(t)|^2\exp\left(-\frac{|\boldsymbol{x}+2\boldsymbol{\theta}L|^2}{r_0^2\left(1+\frac{4L^2}{k_0^2 r_0^4}\right)}\right). \tag{37}$$

The classical diffraction spreading due to the round trip from the surface to the bottom interface and the shift of the envelope of the beam due to the small tilt $\boldsymbol{\theta}$ of the bottom interface are identifiable in (37).

7. Scaling revisited – Explicit representations

In this section we state the assumptions regarding the random medium that allow us to get convenient and explicit expressions for quantities of interest. We remark that the essential scaling assumptions are the scaling of the source, the medium fluctuations and the travel time in terms of the small parameter ε as described in Section 2. We also remark that the expressions for the coherent and incoherent fields and how they depend on the interface depth and tilt can be used for estimation and we will treat this in detail elsewhere. Here, we make some subsequent scaling assumptions that are useful to evaluate the expressions deriving from Proposition 5.1.

We assume that

(a) *the pulse has carrier frequency k_0 and it is narrowband*,
(b) *the input beam spatial profile is Gaussian with radius r_0.*

According to assumptions (a) and (b) we assume the initial conditions

$$f(t,\boldsymbol{x}) = f_0^\delta(t)e^{-ik_0 t}\exp\left(-\frac{|\boldsymbol{x}|^2}{2r_0^2}\right), \quad f_0^\delta(t) = \delta f_0(\delta t), \tag{38}$$

with $\delta \ll 1$ (suppressing the complex conjugate part here and below). We remark that the Gaussian shape assumption serves to simplify expressions, but it is not essential.

We furthermore assume that

(c) *the random fluctuations are statistically isotropic with correlation length l and $l \ll r_0$, moreover, $k_0 r_0 l \sim L$.*

This assumption ensures that diffractive effects are of order one over a propagation distance of order L. We remark that in the random medium case diffractive effects are of order one when $k_0 r_0 l \sim L$. This is when the Rayleigh length associated with the Fresnel length, $\sqrt{r_0 l}$, is of the order of the depth of the slab. Note that in this configuration the random medium fluctuations give an earlier onset of diffractive effects than in the homogeneous case when the Rayleigh length associated with r_0 is of order $k_0 r_0^2$.

We let C_0 and D_0 represent non-dimensionalized quantities so that

$$C(z, \boldsymbol{x}) = \sigma^2 C_0\Big(\frac{z}{l}, \frac{\boldsymbol{x}}{l}\Big), \quad D(\boldsymbol{x}) = \sigma^2 l D_0\Big(\frac{\boldsymbol{x}}{l}\Big).$$

We next assume smooth random medium fluctuations so that the autocovariance function satisfies:

(d) *$D(\boldsymbol{x})$ is at least twice differentiable at $\boldsymbol{x} = \mathbf{0}$ and we can write*

$$D(\boldsymbol{x}) = D(\mathbf{0}) - \frac{\gamma}{2}|\boldsymbol{x}|^2 + o(|\boldsymbol{x}|^2), \quad \gamma = -\frac{1}{d}\Delta D(\mathbf{0}) = \frac{\sigma^2}{l}\gamma_0, \tag{39}$$

with $\gamma_0 = -\Delta D_0(\mathbf{0})/d$.

We introduce the parameter β characterizing the strength of the forward scattering

$$\beta(k_0, L) = L\frac{\sigma^2 k_0^2 l}{4}. \tag{40}$$

Note that β corresponds to the total scattering cross-section and $\beta\hat{D}_0(\cdot)$ a differential scattering cross-section, see (68) and the discussion below. We shall then assume a relatively strong medium interaction:

(e) *$\beta(k_0, L) \gg 1$.*

We remark that this corresponds to $k_0^2 D(\mathbf{0}) L \gg 1$.

The other important parameter that characterizes the microstructure is $\alpha(k_0, L) = L/(k_0 l^2)$. This parameter scales the strength of the diffraction at the scale l of the random fluctuations, see (68). Note that then assumption (c) implies, and is in fact equivalent to,

$$\alpha_0 = \frac{L}{k_0 r_0^2} \ll \alpha_e = \frac{L}{k_0 l r_0} = \mathcal{O}(1) \ll \alpha = \alpha(k_0, L) = \frac{L}{k_0 l^2}.$$

The parameters α_0, α_e and α are inverse Fresnel numbers with the aperture corresponding respectively to the source aperture r_0, random medium effective aperture $\sqrt{l r_0}$ and the medium correlation length l. They describe the strength of diffractive effects for respectively a homogeneous medium with source aperture r_0, the random medium with again source aperture r_0, and a homogeneous medium with source aperture l.

7.1. *Coherent field*

Under (a, b) the limit of the coherent (or mean) reflected field defined by

$$v_{\mathrm{coh},1}(t,\boldsymbol{x}) = \lim_{\varepsilon\to 0} \mathbb{E}\big[v_1^\varepsilon(t,\boldsymbol{x})\big]$$

is given by

$$v_{\mathrm{coh},1}(t,\boldsymbol{x}) = -\mathcal{R}_0 e^{-ik_0 t} f_0^\delta(t) e^{ik_0\boldsymbol{\theta}\cdot\boldsymbol{x}} e^{-\frac{k_0^2}{2}D(\mathbf{0})L} \int \psi_{\mathrm{coh}}(0,\boldsymbol{x}-\boldsymbol{x}') e^{ik\boldsymbol{\theta}\cdot\boldsymbol{x}'} \exp\left(-\frac{|\boldsymbol{x}'|^2}{2r_0^2}\right)\mathrm{d}\boldsymbol{x}',$$

where $\psi_{\mathrm{coh}}(z,\boldsymbol{x})$ is the solution of the Schrödinger equation with damping

$$\frac{\partial\psi_{\mathrm{coh}}}{\partial z} = \frac{i}{k_0}\Delta_{\boldsymbol{x}}\psi_{\mathrm{coh}} - \frac{k_0^2}{4}D(\mathbf{x})\psi_{\mathrm{coh}}$$

starting from $\psi_{\mathrm{coh}}(-L,\boldsymbol{x}) = \delta(\boldsymbol{x})$. Under (a)–(c),

$$\psi_{\mathrm{coh}}(0,\boldsymbol{x}) = \left(\frac{k_0}{4\pi L}\right)^{d/2} e^{-i\frac{\pi d}{4}} \exp\left(-i\frac{k_0|\boldsymbol{x}|^2}{4L}\right),$$

and therefore

$$|v_{\mathrm{coh},1}(t,\boldsymbol{x})|^2 = \mathcal{R}_0^2 e^{-k_0^2 D(\mathbf{0})L} |f_0^\delta(t)|^2 \left(1+\frac{4L^2}{k_0^2 r_0^4}\right)^{-d} \exp\left(-\frac{|\boldsymbol{x}+2\boldsymbol{\theta}L|^2}{r_0^2\left(1+\frac{4L^2}{k_0^2 r_0^4}\right)}\right). \tag{41}$$

This expression is of the form (37) representing the reflected field in the homogeneous case with an exponential damping. If moreover, random scattering is strong, assumption (e), then the coherent field is vanishing.

7.2. *Incoherent field*

Under (a)–(c), the coherence function of the reflected field defined by

$$A_1(s,t,\boldsymbol{x},\boldsymbol{y}) = \lim_{\varepsilon\to 0} \mathbb{E}\left[v_1^\varepsilon\left(s+\frac{t}{2},\boldsymbol{x}+\frac{\boldsymbol{y}}{2}\right)\overline{v_1^\varepsilon}\left(s-\frac{t}{2},\boldsymbol{x}-\frac{\boldsymbol{y}}{2}\right)\right] \tag{42}$$

has the form

$$\begin{aligned} A_1(s,t,\boldsymbol{x},\boldsymbol{y}) = {} & \mathcal{R}_0^2 f_0^\delta\left(s+\frac{t}{2}\right)\overline{f_0^\delta}\left(s-\frac{t}{2}\right) e^{-ik_0 t} e^{2ik_0\boldsymbol{\theta}\cdot\boldsymbol{y}} \\ & \times \left(\frac{r_0}{2\sqrt{\pi}}\right)^d \int e^{-\frac{r_0^2|\boldsymbol{\eta}|^2}{4} - \frac{|\boldsymbol{y}|^2}{4r_0^2}} e^{-i\boldsymbol{\eta}\cdot\boldsymbol{x} - 2iL\boldsymbol{\theta}\cdot\boldsymbol{\eta}} e^{\frac{k_0^2}{4}\int_0^{2L} D\left(\boldsymbol{\eta}\frac{z}{k_0}+\boldsymbol{y}\right) - D(\mathbf{0})\mathrm{d}z} \mathrm{d}\boldsymbol{\eta}. \end{aligned} \tag{43}$$

We give the details of the derivation of this result in Appendix 1.

If moreover, random scattering is strong, assumption (e), and the random medium fluctuations are smooth, assumption (d), then we obtain that the coherence

function has the Gaussian shape

$$A_1(s,t,\boldsymbol{x},\boldsymbol{y}) = \mathcal{R}_0^2 f_0^\delta\Big(s+\frac{t}{2}\Big)\overline{f_0^\delta}\Big(s-\frac{t}{2}\Big)e^{-ik_0 t}\Big(\frac{r_0}{r_R(L)}\Big)^d \times \exp\Big(-\frac{|\boldsymbol{x}+2\boldsymbol{\theta}L|^2}{r_R(L)^2} - \frac{|\boldsymbol{y}|^2}{4\rho_R(L)^2} + i\frac{(\boldsymbol{x}+2\boldsymbol{\theta}L)\cdot\boldsymbol{y}}{\chi_R(L)^2} + i2k_0\boldsymbol{\theta}\cdot\boldsymbol{y}\Big). \quad (44)$$

The beam radius $r_R(L)$, the correlation radius $\rho_R(L)$, and the parameter $\chi_R(L)$ are characterized by

$$r_R(L) = r_0\sqrt{1+\frac{4\gamma L^3}{3r_0^2}}, \quad (45)$$

$$\rho_R(L) = r_0\frac{\sqrt{1+\frac{4\gamma L^3}{3r_0^2}}}{\sqrt{1+k_0^2r_0^2\gamma L+\frac{k_0^2\gamma^2L^4}{3}}}, \quad (46)$$

$$\chi_R(L) = \frac{r_R(L)}{\sqrt{k_0\gamma L^2}}, \quad (47)$$

where we have taken into account that $k_0r_0^2 \gg L$ in the considered regime. The correlation radius $\rho_R(L)$ of the reflected field describes the lateral separation at which the field decorrelates and hence its scale of variation. Thus, the field amplitude has transverse random fluctuations at the scale of the correlation radius $\rho_R(L)$ within an overall envelope whose width is $r_R(L)$. It is seen that the correlation radius is small relative to the initial lateral support of the source, that is r_0, in our scaling regime. The same holds true for the parameter $\chi_R(L)$ which describes a scale of phase decoherence of the reflected field.

Note that we can write respectively

$$\frac{\gamma L^3}{4r_0^2} = \gamma_0\alpha_e\beta, \quad \frac{4\gamma L^3}{r_0^2}\frac{1}{k_0^2\gamma^2L^4} = \frac{1}{\gamma_0}\frac{(l/r_0)^2}{\beta}, \quad \frac{\gamma L^3}{r_0^2}\frac{1}{k_0\gamma L^2} = \alpha_0,$$

so that in our scaling regime

$$\frac{r_R(L)}{r_0} \gg 1, \quad \frac{\rho_R(L)}{r_0} \ll 1, \quad \frac{\chi_R(L)}{r_0} \ll 1,$$

respectively. In the regime that we consider it is not possible to observe in the spatial coherence function (42) any coherent effect building up between the forward and backward propagations. In fact, one can check that the expressions for the beam radius r_R and correlation radius ρ_R coincide to leading order to the ones that we would have obtained by considering propagation through independent random medium realizations in the transmission and reflection directions of propagation [3]. However, there is an interesting coherence phenomenon that can be observed in a small angular cone and we discuss the so-called enhanced backscattering phenomenon in the next section.

8. Enhanced backscattering

In this section, we show that the reflected intensity exhibits a singular picture in a very narrow cone (in lateral slowness $\boldsymbol{\kappa}$), of angular width of order α^{-1}, around the backscattered direction. This phenomenon, called enhanced backscattering or weak localization, is widely discussed in the physics literature [5,6] and it has been observed in several experimental contexts [8–11]. We remark that we here consider enhanced backscattering as associated with a random medium rather than with a rough surface as discussed in for instance [12]. Enhanced backscattering can be described as follows: Let a quasi-monochromatic quasi-plane wave be incident with a certain angle. Then the mean reflected power has a local maximum in the backscattered direction, which is twice as large as the mean reflected power in the other directions. In this section, we give a mathematical proof of enhanced backscattering and we deduce the maximum, the angular width, and the shape of the enhanced backscattering cone.

8.1. *Enhanced backscattering from a strong interface*

We assume that the incoming wave is generated by a source function with

$$f(t,\boldsymbol{x}) = f_0^{\delta}(t)e^{-ik_0 t}g_{\mathrm{inc}}(\boldsymbol{x})$$

representing an incident beam. Here, f is narrowband as before, while $\hat{\mathrm{g}}_{\mathrm{inc}}(\boldsymbol{\kappa})$ is concentrated at some $\boldsymbol{\kappa}_{\mathrm{inc}}$. Essentially, $f(t,\boldsymbol{x})$ is a wave packet as before, oriented in a direction corresponding with an incident direction of propagation determined by $\boldsymbol{\kappa}_{\mathrm{inc}}$. The scaling is such that the angular width of the incoming beam is smaller than α^{-1}.

The first reflected constituent in the direction $\boldsymbol{\kappa}_0$ is

$$\widetilde{v}_1^{\varepsilon}(s,\boldsymbol{\kappa}_0) = \int v_1^{\varepsilon}(s,\boldsymbol{x})e^{-i\boldsymbol{\kappa}_0\cdot\boldsymbol{x}}\,\mathrm{d}\boldsymbol{x}.$$

From (26)–(28) it follows that

$$\widetilde{v}_1^{\varepsilon}(s,\boldsymbol{\kappa}_0) = -\frac{1}{2\pi}\int\int \widetilde{\boldsymbol{\mathcal{R}}}^{\varepsilon}(k+k_0,0,\boldsymbol{x},\boldsymbol{x}')e^{i(k+k_0)(\boldsymbol{\theta}\cdot\boldsymbol{x}+\boldsymbol{\theta}\cdot\boldsymbol{x}')}\hat{f}\left(\frac{k}{\delta}\right)g_{\mathrm{inc}}(\boldsymbol{x}')\mathrm{d}\boldsymbol{x}' \times e^{-i(k+k_0)s}\,\mathrm{d}k e^{-i\boldsymbol{\kappa}_0\cdot\boldsymbol{x}}\,\mathrm{d}\boldsymbol{x}.$$

We then find that

$$\widetilde{v}_1^{\varepsilon}(s,\boldsymbol{\kappa}_0) = -\frac{1}{2\pi}\int\int \widehat{\boldsymbol{\mathcal{R}}}^{\varepsilon}(k+k_0,0,\boldsymbol{\kappa}_0-(k+k_0)\boldsymbol{\theta},\boldsymbol{\kappa}'+(k+k_0)\boldsymbol{\theta})\hat{f}\left(\frac{k}{\delta}\right)\hat{g}_{\mathrm{inc}}(\boldsymbol{\kappa}') \times e^{-i(k+k_0)s}\,\mathrm{d}k\,\mathrm{d}\boldsymbol{\kappa}'. \tag{48}$$

The mean of the square modulus of $\widetilde{v}_1^{\varepsilon}(s,\boldsymbol{\kappa}_0)$ only involves the mean of the product of a pair of reflection kernels, and it follows that this mean converges to the mean of the square modulus of the limit process $\widetilde{v}_1(s,\boldsymbol{\kappa}_0)$ defined as the Fourier transform in $\boldsymbol{x}$ of $v_1(s,\boldsymbol{x})$ given by (30) [3]. This means that the mean reflected

intensity in the direction $\boldsymbol{\kappa}_0$ satisfies

$$\lim_{\varepsilon\to 0}\mathbb{E}\big[|\widetilde{v}_1^{\varepsilon}(s,\boldsymbol{\kappa}_0)|^2\big]=\mathcal{R}_0^2|f_0^{\delta}(s)|^2I^R(\boldsymbol{\kappa}_0),$$
$$I^R(\boldsymbol{\kappa}_0)=2^{-d}l_x^d\int\mathcal{V}^{\mathrm{R}}\bigg(1,\frac{\boldsymbol{\kappa}_0-\boldsymbol{\kappa}_1'-2k_0\boldsymbol{\theta}}{2}l,(\boldsymbol{\kappa}_0+\boldsymbol{\kappa}_1')l,\mathbf{0}\bigg)|\hat{g}_{\mathrm{inc}}(\boldsymbol{\kappa}_1')|^2\,\mathrm{d}\boldsymbol{\kappa}_1'. \tag{49}$$

Here $\mathcal{V}_{\mathrm{R}}$ is a transformed Wigner transform and is introduced in Appendix 2. We derive this result in Appendix 3. Using the fact that $\hat{\mathrm{g}}_{\mathrm{inc}}(\boldsymbol{\kappa})$ is concentrated at $\boldsymbol{\kappa}_{\mathrm{inc}}$, we get

$$I^R(\boldsymbol{\kappa}_0)\simeq P_{\mathrm{inc}}\mathcal{V}^{\mathrm{R}}\bigg(1,\frac{\boldsymbol{\kappa}_0-(\boldsymbol{\kappa}_{\mathrm{inc}}+2k_0\boldsymbol{\theta})}{2}l,(\boldsymbol{\kappa}_0+\boldsymbol{\kappa}_{\mathrm{inc}})l,\mathbf{0}\bigg), \tag{50}$$

where $P_{\mathrm{inc}}=2^{-d}l_x^d\int|\hat{g}_{\mathrm{inc}}(\boldsymbol{\kappa}_1')|^2\,\mathrm{d}\boldsymbol{\kappa}_1'$. This formula gives the mean reflected intensity in the direction $\boldsymbol{\kappa}_0$ and is valid for arbitrary values of α and β.

We consider the regime $\alpha\gg 1$. The mean reflected intensity, far enough from the backscattered direction $-\kappa_{\mathrm{inc}}$, that is, for $|\kappa_0+\kappa_{\mathrm{inc}}|l\gg\alpha^{-1}$, is of the form

$$\begin{aligned}I^R(\boldsymbol{\kappa}_0)&=P_{\mathrm{inc}}\mathcal{V}_{\mathbf{0}}^{\mathrm{R}}\bigg(1,\frac{\boldsymbol{\kappa}_0-(\boldsymbol{\kappa}_{\mathrm{inc}}+2k_0\boldsymbol{\theta})}{2}l\bigg)\\&=\frac{P_{\mathrm{inc}}}{(2\pi)^d}\int e^{-il(\boldsymbol{\kappa}_0-(\boldsymbol{\kappa}_{\mathrm{inc}}+2k_0\boldsymbol{\theta}))\cdot\boldsymbol{u}/2}e^{2\beta(D_0(\frac{\boldsymbol{u}}{2})-D_0(\mathbf{0}))}\,\mathrm{d}\boldsymbol{u},\end{aligned} \tag{51}$$

where we used the second statement of Lemma 2.1. In a narrow angular cone around the backscattered direction $-\kappa_{\mathrm{inc}}$, the reflected intensity is locally larger:

$$\begin{aligned}I^R(-\boldsymbol{\kappa}_{\mathrm{inc}}+\alpha^{-1}\boldsymbol{\kappa})&=P_{\mathrm{inc}}\big[\mathcal{V}_{\mathbf{0}}^{\mathrm{R}}(1,\,-(\boldsymbol{\kappa}_{\mathrm{inc}}+k_0\boldsymbol{\theta})l)+\mathcal{V}_{\boldsymbol{\kappa}l}^{\mathrm{R}}(1,\,-(\boldsymbol{\kappa}_{\mathrm{inc}}+k_0\boldsymbol{\theta})l)\big]\\&=\frac{P_{\mathrm{inc}}}{(2\pi)^d}\bigg[\int e^{il(\boldsymbol{\kappa}_{\mathrm{inc}}+k_0\boldsymbol{\theta})\cdot\boldsymbol{u}}e^{2\beta(D_0(\frac{\boldsymbol{u}}{2})-D_0(\mathbf{0}))}\,\mathrm{d}\boldsymbol{u}\\&\quad+\int e^{il(\boldsymbol{\kappa}_{\mathrm{inc}}+k_0\boldsymbol{\theta})\cdot\boldsymbol{u}}e^{\beta\int_{-1}^{1}D_0(\frac{\boldsymbol{u}}{2}+\boldsymbol{\kappa}l\zeta')-D_0(\mathbf{0})\mathrm{d}\zeta'}\,\mathrm{d}\boldsymbol{u}\bigg],\end{aligned} \tag{52}$$

where we used the third statement of Lemma 2.1. Note that in the regime of $\beta\ll 1$ we see from (51) that we have sharp specular reflection in the direction $\boldsymbol{\kappa}_{\mathrm{inc}}+2k_0\boldsymbol{\theta}$ and from (52) that the enhanced backscattering cone vanishes in this limit. If we assume that $\beta\gg 1$, then the main contribution to the integral in (51) is concentrated to small $|\boldsymbol{u}|$ and we can replace

$$e^{2\beta(D_0(\frac{\boldsymbol{u}}{2})-D_0(\mathbf{0}))}\approx e^{\beta\Delta D_0(\mathbf{0})|\boldsymbol{u}|^2/(4d)}=e^{-\beta\gamma_0|\boldsymbol{u}|^2/4},$$

so that

$$I^R(\boldsymbol{\kappa}_0)=\frac{P_{\mathrm{inc}}}{(\pi\gamma_0\beta)^{d/2}}\exp\bigg(-\frac{|\boldsymbol{\kappa}_0-(\boldsymbol{\kappa}_{\mathrm{inc}}+2k_0\boldsymbol{\theta})|^2l^2}{4\gamma_0\beta}\bigg), \tag{53}$$

again, for $|\boldsymbol{\kappa}_0+\boldsymbol{\kappa}_{\rm inc}|l\gg\alpha^{-1}$, where γ_0 is the dimensionless version of γ given by (39): $\gamma=\sigma^2 l^{-1}\gamma_0$. This formula gives the width of the diffusive cone around the "specular direction" $\boldsymbol{\kappa}_{\rm inc}+2k_0\boldsymbol{\theta}$:

$$\Delta\kappa_{\rm spec}=\frac{2\sqrt{\gamma_0\beta}}{l}=\sqrt{\gamma L}k_0=\frac{2}{\rho_R(L)}. \tag{54}$$

This implies that a rapid decorrelation of the reflected field corresponds to a diffuse and broad specular cone.

On the top of this broad cone, we have a narrow cone of relative maximum equal to 2 centered along the backscattered direction $-\boldsymbol{\kappa}_{\rm inc}$:

$$I^R(-\boldsymbol{\kappa}_{\rm inc}+\alpha^{-1}\boldsymbol{\kappa})=\frac{P_{\rm inc}}{(\pi\gamma_0\beta)^{d/2}}\exp\left(-\frac{|\boldsymbol{\kappa}_{\rm inc}+k_0\boldsymbol{\theta}|^2 l^2}{\gamma_0\beta}\right)\left[1+\exp\left(-\frac{\gamma_0\beta}{3}|\boldsymbol{\kappa}|^2 l^2\right)\right]. \tag{55}$$

This shows that the width of the enhanced backscattering cone is

$$\Delta\kappa_{\rm EBC}=\frac{\sqrt{3}}{l\sqrt{\gamma_0\beta}\alpha}=\frac{2\sqrt{3}}{\sqrt{\gamma L^3}}=\frac{4}{r_R(L)}. \tag{56}$$

Therefore, a wide broadening of the reflected wave energy goes with a relatively sharp enhanced backscattering cone. We remark that the results (53) and (55) are based on the assumption of a smooth correlation function, assumption (*d*); indeed, then the shapes of the specular and backscattering cones are smooth in general and Gaussian when $\beta\gg 1$. Note also that the enhancement can be seen when the source is concentrated in wave vector so that the angular width of the incoming beam is smaller than α^{-1}. In the case of a parabolic beam with an angular width of order one the coherence between the downward and upward paths is no longer focused to a narrow angular cone and the enhanced backscattering becomes lower order. In the case when the backscattering comes from the medium fluctuations only, then the shapes of the specular and backscattering cones depend sensitively on the roughness of the medium. In particular the backscattering cone can have a cusp for rough media [7]. Note that the angular width of the backscattering cone

$$\Delta\theta_{\rm EBC}=\frac{\Delta\kappa_{\rm EBC}}{k_0}=\frac{4}{k_0 r_R(L)} \tag{57}$$

is proportional to the wavelength, as predicted by physical arguments based on diagrammatic expansions [6].

We remark that the reciprocal relation to the beam spreading is also in agreement with the physical interpretation of enhanced backscattering as a constructive interference between pairs of wave "paths" and reversed paths (see Figure 2). The sum of all these constructive interferences should give an enhancement factor of 2 in the backscattered direction as follows from the following heuristic argument. Assume that the reflected wave is observed with an angle A. For paths corresponding to $A=0$ there are two perfectly correlated paths, while for A large they become independent. The factor of 2 then corresponds to the variance of two perfectly correlated random variables relative to the variance when they are independent. Note that the cone of correlated directions then will give the width of the enhanced

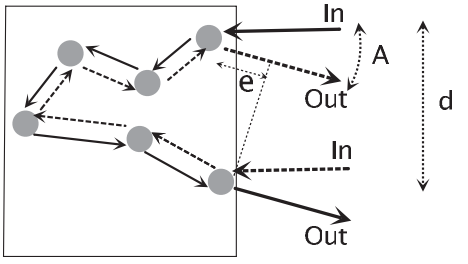

Figure 2. Physical interpretation of the scattering of a plane wave by a random medium. The output wave in direction A is the superposition of many different scattering paths. One of these paths is plotted as well as the reversed path. The phase difference between the two outgoing waves is $ke = kd \sin A$.

backscattering cone. Now, if the reflected wave is observed with an angle A compared to the backscattered direction, then the phase shift between the direct and reversed paths is $ke = kd \sin A$, where d is the typical transverse size of a wave path, which is in our setting of the order of the beam width r_R. Therefore, constructive interference is possible in the approximate range $k_0 r_R A \leq \pi$, which gives the angular aperture of the enhanced backscattering cone. This "path" interpretation is not used in our paper, but we recover the physical result by exploiting our Itô–Schrödinger model.

8.2. *Enhanced backscattering from a diffusive interface*

We discuss in this subsection the enhanced backscattering cone in the case of a diffusive interface, and show that it is robust with respect to such a model generalization. In the previous sections we considered the case of a specular reflection at a homogeneous interface. Here, we revisit the analysis in the case in which an inhomogeneous interface is inserted in the plane $z = -L - \varepsilon^2 \boldsymbol{\theta} \cdot x$, with impedance $Z_M(\boldsymbol{x}/\varepsilon^2)$, so that the second boundary condition (11) attains the form

$$\widetilde{a}^{\varepsilon}(k, -L, \boldsymbol{x}) e^{-ik\frac{L}{\varepsilon^4}} - R_M(\boldsymbol{x}) \widetilde{b}^{\varepsilon}(k, -L, \boldsymbol{x}) e^{ik\frac{L}{\varepsilon^4}} = 0,$$

where $R_M(\boldsymbol{x}) = (Z_M(\boldsymbol{x}) - 1)/(Z_M(\boldsymbol{x}) + 1)$ is the local reflection coefficient of the interface. In this case, the initial condition at $z = -L$ for the reflection operator is

$$\widetilde{\boldsymbol{\mathcal{R}}}^{\varepsilon}(k, -L, \boldsymbol{x}, \boldsymbol{x}') = R_M(\boldsymbol{x}) \delta(\boldsymbol{x} - \boldsymbol{x}').$$

We assume here that R_M is a stationary random process, with mean zero and autocovariance function

$$\mathbb{E}[R_M(\boldsymbol{x}) \overline{R_M}(\boldsymbol{x}')] = R_0^2 \psi(\boldsymbol{x} - \boldsymbol{x}').$$

We can repeat the arguments of Appendix 3 and find that the reflected intensity is still given by (50). In fact the only change is in the initial condition for the transformed Wigner transform $\mathcal{V}^R$. The enhanced backscattering cone can then be found by an argument as in the previous section, using the results of Lemma 2.2 rather than Lemma 2.1.

Now the mean reflected intensity, far enough from the backscattered direction $-\boldsymbol{\kappa}_{\rm inc}$, that is, for $|\boldsymbol{\kappa}_0+\boldsymbol{\kappa}_{\rm inc}|l\gg\alpha^{-1}$, is of the form

$$I^R(\boldsymbol{\kappa}_0)=\frac{P_{\rm inc}}{(2\pi)^d}\int\psi\left(\frac{l\boldsymbol{u}}{2}\right)e^{-il(\boldsymbol{\kappa}_0-(\boldsymbol{\kappa}_{\rm inc}+2k_0\boldsymbol{\theta}))\cdot\boldsymbol{u}/2}e^{2\beta(D_0(\frac{\boldsymbol{u}}{2})-D_0(\boldsymbol{0}))}\,{\rm d}\boldsymbol{u}, \tag{58}$$

where we have used the second statement of Lemma 2.2. To get simple explicit expressions for the characteristics of the reflected wave we assume that ψ is Gaussian:

$$\psi(\boldsymbol{x})=e^{-\frac{|\boldsymbol{x}|^2}{a^2}}, \tag{59}$$

where a is the correlation radius of the diffusive interface. We then find when $\beta\gg1$ that

$$I^R(\boldsymbol{\kappa}_0)=\frac{P_{\rm inc}}{(\pi(\gamma_0\beta+(l/a)^2)^{d/2}}\exp\left(-\frac{|\boldsymbol{\kappa}_0-(\boldsymbol{\kappa}_{\rm inc}+2k_0\boldsymbol{\theta})|^2l^2}{4(\gamma_0\beta+(l/a)^2)}\right), \tag{60}$$

again, for $|\boldsymbol{\kappa}_0+\boldsymbol{\kappa}_{\rm inc}|l\gg\alpha^{-1}$. This formula gives the width of the diffusive cone around the "specular direction" $\boldsymbol{\kappa}_{\rm inc}+2k_0\boldsymbol{\theta}$:

$$\Delta\kappa^a_{\rm spec}=\frac{2\sqrt{\gamma_0\beta+(l/a)^2}}{l}=k_0\sqrt{\gamma L+4/(ak_0)^2}, \tag{61}$$

which shows that the diffusive interface broadens the specular cone and the angular broadening becomes strong when $k_0a\ll1$. Correspondingly, in a narrow angular cone around the backscattered direction $-\boldsymbol{\kappa}_{\rm inc}$, the reflected intensity is locally larger, now given by:

$$\begin{aligned}I^R(-\boldsymbol{\kappa}_{\rm inc}+\alpha^{-1}\boldsymbol{\kappa})=\frac{P_{\rm inc}}{(2\pi)^d}\Bigg[&\int\psi\left(\frac{l\boldsymbol{u}}{2}\right)e^{il(\boldsymbol{\kappa}_{\rm inc}+k_0\boldsymbol{\theta})\cdot\boldsymbol{u}}e^{2\beta(D_0(\frac{\boldsymbol{u}}{2})-D_0(\boldsymbol{0}))}\,{\rm d}\boldsymbol{u}\\&+\int\psi\left(\frac{l\boldsymbol{u}}{2}\right)e^{il(\boldsymbol{\kappa}_{\rm inc}+k_0\boldsymbol{\theta})\cdot\boldsymbol{u}}e^{\beta\int_{-1}^{1}D_0(\frac{\boldsymbol{u}}{2}+\boldsymbol{\kappa}l\zeta')-D_0(\boldsymbol{0}){\rm d}\zeta'}\,{\rm d}\boldsymbol{u}\Bigg],\end{aligned}$$

where we have used the third statement of Lemma 2.2. It then again follows that, when $\beta\gg1$, on the top of the broad cone, we have a narrow cone of relative maximum equal to 2 centered along the backscattered direction $-\boldsymbol{\kappa}_{\rm inc}$:

$$\begin{aligned}I^R(-\boldsymbol{\kappa}_{\rm inc}+\alpha^{-1}\boldsymbol{\kappa})=&\frac{P_{\rm inc}}{(\pi(\gamma_0\beta+(l/a)^2)^{d/2}}\exp\left(-\frac{|\boldsymbol{\kappa}_{\rm inc}+k_0\boldsymbol{\theta}|^2l^2}{\gamma_0\beta+(l/a)^2}\right)\\&\times\left[1+\exp\left(-\frac{\gamma_0\beta}{3}|\boldsymbol{\kappa}|^2l^2\right)\right].\end{aligned} \tag{62}$$

We observe that the relative magnitude and width of the cone are not affected by the replacement of the specular interface with a diffusive interface.

9. Conclusions

We analyzed multiple reflections from a random slab terminating in a tilted interface and with pressure release boundary conditions on top. The tilt is relatively small so

that we can retain the overall slab geometry but it is non-negligible in that it produces a deviation in the specular reflection of a normally incident beam of the order of the beam width. We use an invariant imbedding formulation and a representation of the associated reflection and transmission operators in terms of Itô–Schrödinger equations to obtain a description of the wave field statistics. The thickness of the slab is large enough so that the waves transmitted through and reflected by the random medium are partly coherent. In other words the thickness of the slab is of the order of the mean free path. We use this representation in particular to analyze the correlation structure of the transmitted field and the structure of the enhanced backscattering cone. From a physics point of view, the cone arises as a coherence phenomenon and hence one could expect that the cone will be independent of the small tilt of the bottom interface; indeed, this is confirmed by our analysis. Moreover, the cone is not affected by making the terminating interface diffuse which again can be understood in that the cone comes from coherence in retro-reflected paths. The angular width of the cone is proportional to the ratio of the wavelength over the beam width. Since the beam width is enhanced by scattering by the random medium this shows that strong medium fluctuations and a relatively deep slab gives a narrow cone. This result holds as long as the Itô–Schrödinger equations are valid, which means that the beam width should remain smaller than the interface depth, and as long as the tilt is not too large, otherwise the backscattered direction is not in the diffusive specular cone and the enhanced backscattering peak is too small to be observable.

Acknowledgements

The work was partially supported by NSF ARRA grant DMS 0908274 and by ERC Advanced Grant Project MULTIMOD-267184.

References

[1] A. Bamberger, B. Engquist, L. Halpern, and P. Joly, *Parabolic wave equation approximations in heterogeneous media*, SIAM J. Appl. Math. 48 (1988), pp. 99–128.
[2] C. Bernardi and M.-C. Pelissier, *Spectral approximation of a Schrödinger type equation*, Math. Models Methods Appl. Sci. 4 (1994), pp. 49–88.
[3] J. Garnier and K. Sølna, *Coupled paraxial wave equations in random media in the white-noise regime*, Ann. Appl. Probab. 19 (2009), pp. 318–346.
[4] D. Dawson and G. Papanicolaou, *A random wave process*, Appl. Math. Optim. 12 (1984), pp. 97–114.
[5] Y.N. Barabanenkov, *Wave corrections for the transfer equation for backward scattering*, Izv. Vyssh. Uchebn. Zaved. Radiofiz. 16 (1973), pp. 88–96.
[6] M.C.W. van Rossum and Th.M. Nieuwenhuizen, *Multiple scattering of classical waves: microscopy, mesoscopy, and diffusion*, Rev. Mod. Phys. 71 (1999), pp. 313–371.
[7] J. Garnier and K. Sølna, *Random backscattering in the parabolic scaling*, J. Stat. Phys. 131 (2008), pp. 445–486.
[8] P.E. Wolf and G. Maret, *Weak localization and coherent backscattering of photons in disordered media*, Phys. Rev. Lett. 55 (1985), pp. 2696–2699.
[9] M.P. van Albada and A. Lagendijk, *Observation of weak localization of light in a random medium*, Phys. Rev. Lett. 55 (1985), pp. 2692–2695.

[10] A. Tourin, A. Derode, P. Roux, B.A. van Tiggelen, and M. Fink, *Time-dependent coherent backscattering of acoustic waves*, Phys. Rev. Lett. 79 (1997), pp. 3637–3639.
[11] G. Labeyrie, F. de Tomasi, J.-C. Bernard, C.A. Müller, C. Miniatura, and R. Kaiser, *Coherent backscattering of light by atoms*, Phys. Rev. Lett. 83 (1999), pp. 5266–5269.
[12] Z.H. Gu, J. Lu, and A.A. Maradudin, *Enhanced backscattering from a rough dielectric film on a glass substrate*, J. Opt. Soc. Am. A. 10 (1993), pp. 1753–1764.

Appendix 1. Coherence function of the reflected wave

We derive expression (43) for the form of the coherence function of the reflected wave defined by (42). We find using (30) that

$$A_1(s,t,\boldsymbol{x},\boldsymbol{y}) = \frac{1}{(2\pi)^2}\int\int \mathbb{E}\left[\widetilde{\boldsymbol{\mathcal{R}}}\left(k,0,\boldsymbol{x}+\frac{\boldsymbol{y}}{2},\boldsymbol{x}'\right)\overline{\widetilde{\boldsymbol{\mathcal{R}}}\left(k,0,\boldsymbol{x}-\frac{\boldsymbol{y}}{2},\boldsymbol{x}''\right)}\right] \times e^{ik\boldsymbol{\theta}\cdot(\boldsymbol{x}+\frac{\boldsymbol{y}}{2}+\boldsymbol{x}')}\widetilde{f}^{\delta}(k,\boldsymbol{x}')\mathrm{d}\boldsymbol{x}' e^{-ik(s+\frac{t}{2})}\,\mathrm{d}k e^{-ik'\boldsymbol{\theta}\cdot(\boldsymbol{x}-\frac{\boldsymbol{y}}{2}+\boldsymbol{x}'')}\overline{\widetilde{f}^{\delta}(k',\boldsymbol{x}'')}\mathrm{d}\boldsymbol{x}'' e^{ik'(s-\frac{t}{2})}\,\mathrm{d}k'.$$

We note that

$$\widetilde{f}^{\delta}(k,\boldsymbol{x}) = e^{-\frac{|\boldsymbol{x}|^2}{2r_0^2}}\hat{f}\left(\frac{k-k_0}{\delta}\right).$$

In view of the narrow bandwidth assumption we then get

$$\begin{aligned} A_1(s,t,\boldsymbol{x},\boldsymbol{y}) &= \frac{1}{(2\pi)^2}\int\int \mathbb{E}\left[\widetilde{\boldsymbol{\mathcal{R}}}\left(k_0,0,\boldsymbol{x}+\frac{\boldsymbol{y}}{2},\boldsymbol{x}'\right)\overline{\widetilde{\boldsymbol{\mathcal{R}}}\left(k_0,0,\boldsymbol{x}-\frac{\boldsymbol{y}}{2},\boldsymbol{x}''\right)}\right] e^{-\frac{|\boldsymbol{x}'|^2}{2r_0^2}} e^{-\frac{|\boldsymbol{x}''|^2}{2r_0^2}} \\ &\quad\times \hat{f}\left(\frac{k}{\delta}\right)\bar{\hat{f}}\left(\frac{k'}{\delta}\right)e^{ik_0\boldsymbol{\theta}\cdot(\boldsymbol{x}'-\boldsymbol{x}''+\boldsymbol{y}-t)}e^{-i(k+k')t/2}e^{-i(k-k')s}\,\mathrm{d}k\,\mathrm{d}k'\,\mathrm{d}\boldsymbol{x}'\,\mathrm{d}\boldsymbol{x}'' \\ &= \int\int \mathbb{E}\left[\widetilde{\boldsymbol{\mathcal{R}}}\left(k_0,0,\boldsymbol{x}+\frac{\boldsymbol{y}}{2},\boldsymbol{x}'\right)\overline{\widetilde{\boldsymbol{\mathcal{R}}}\left(k_0,0,\boldsymbol{x}-\frac{\boldsymbol{y}}{2},\boldsymbol{x}''\right)}\right] e^{\frac{|\boldsymbol{x}'|^2+|\boldsymbol{x}''|^2}{2r_0^2}} \\ &\quad\times f_0^{\delta}(s+t/2)\overline{f_0^{\delta}(s-t/2)}e^{ik_0(\boldsymbol{\theta}\cdot(\boldsymbol{x}'-\boldsymbol{x}''+\boldsymbol{y})-t)}\,\mathrm{d}\boldsymbol{x}'\,\mathrm{d}\boldsymbol{x}''. \end{aligned}$$

In order to characterize the coherence function A_1 we introduce the Wigner transform of the reflection operator defined by

$$\begin{aligned} W_k^R(z,\boldsymbol{x},\boldsymbol{x}',\boldsymbol{\kappa},\boldsymbol{\kappa}') = \int\int e^{-i(\boldsymbol{\kappa}\cdot\boldsymbol{y}+\boldsymbol{\kappa}'\cdot\boldsymbol{y}')}\mathbb{E}\Bigg[&\widetilde{\boldsymbol{\mathcal{R}}}\left(k,\,-z,\boldsymbol{x}+\frac{\boldsymbol{y}}{2},\boldsymbol{x}'+\frac{\boldsymbol{y}'}{2}\right) \\ &\times\overline{\widetilde{\boldsymbol{\mathcal{R}}}\left(k,\,-z,\boldsymbol{x}-\frac{\boldsymbol{y}}{2},\boldsymbol{x}'-\frac{\boldsymbol{y}'}{2}\right)}\Bigg]\mathrm{d}\boldsymbol{y}\,\mathrm{d}\boldsymbol{y}'. \end{aligned} \tag{63}$$

It satisfies a set of transport equations:

$$\begin{aligned} \frac{\partial W_k^R}{\partial z}+\frac{\boldsymbol{\kappa}}{k}\cdot\nabla_{\boldsymbol{x}}W_k^R+\frac{\boldsymbol{\kappa}'}{k}\cdot\nabla_{\boldsymbol{x}'}W_k^R = \frac{k^2}{4(2\pi)^d}\int\hat{D}(\boldsymbol{u})\Bigg[&W_k^R(z,\boldsymbol{x},\boldsymbol{x}',\boldsymbol{\kappa}-\boldsymbol{u},\boldsymbol{\kappa}')+W_k^R(z,\boldsymbol{x},\boldsymbol{x}',\boldsymbol{\kappa},\boldsymbol{\kappa}'-\boldsymbol{u}) \\ &+2W_k^R\left(z,\boldsymbol{x},\boldsymbol{x}',\boldsymbol{\kappa}-\frac{1}{2}\boldsymbol{u},\boldsymbol{\kappa}'-\frac{1}{2}\boldsymbol{u}\right)\cos(\boldsymbol{u}\cdot(\boldsymbol{x}-\boldsymbol{x}')) \\ &-2W_k^R\left(z,\boldsymbol{x},\boldsymbol{x}',\boldsymbol{\kappa}-\frac{1}{2}\boldsymbol{u},\boldsymbol{\kappa}'+\frac{1}{2}\boldsymbol{u}\right)\cos(\boldsymbol{u}\cdot(\boldsymbol{x}-\boldsymbol{x}')) \\ &-2W_k^R(z,\boldsymbol{x},\boldsymbol{x}',\boldsymbol{\kappa},\boldsymbol{\kappa}')\Bigg]\mathrm{d}\boldsymbol{u}, \end{aligned} \tag{64}$$

starting from $W_k^R(z=L,\boldsymbol{x},\boldsymbol{x}',\boldsymbol{\kappa},\boldsymbol{\kappa}')=(2\pi)^d\mathcal{R}_0^2\delta(\boldsymbol{x}-\boldsymbol{x}')\delta(\boldsymbol{\kappa}+\boldsymbol{\kappa}')$. The coherence function can now be expressed as

$$\begin{aligned}A_1(s,t,\boldsymbol{x},\boldsymbol{y})&=\mathcal{H}(\boldsymbol{x},\boldsymbol{y})\mathcal{R}_0^2 f_0^\delta(s+t/2)\overline{f_0^\delta(s-t/2)}e^{ik_0(\boldsymbol{\theta}\cdot\boldsymbol{y}-t)},\\ \mathcal{H}(\boldsymbol{x},\boldsymbol{y})&=\frac{1}{(2\pi)^{2d}\mathcal{R}_0^2}\int\int W_{k_0}^R\left(0,\boldsymbol{x},\frac{\boldsymbol{x}'+\boldsymbol{x}''}{2},\boldsymbol{\kappa},\boldsymbol{\kappa}'\right)e^{i(\boldsymbol{\kappa}\cdot\boldsymbol{y}+\boldsymbol{\kappa}'\cdot(\boldsymbol{x}'-\boldsymbol{x}''))}\,\mathrm{d}\boldsymbol{\kappa}\,\mathrm{d}\boldsymbol{\kappa}'\\ &\quad\times e^{-\frac{|\boldsymbol{x}'|^2+|\boldsymbol{x}''|^2}{2r_0^2}}e^{ik_0\boldsymbol{\theta}\cdot(\boldsymbol{x}'-\boldsymbol{x}'')}\,\mathrm{d}\boldsymbol{x}'\,\mathrm{d}\boldsymbol{x}''.\end{aligned}\tag{65}$$

From (66) and (67) we have

$$\begin{aligned}W_k^R(0,\boldsymbol{x},\boldsymbol{x}',\boldsymbol{\kappa},\boldsymbol{\kappa}')&=\mathcal{R}_0^2(l/2)^d\int e^{i\boldsymbol{\kappa}''\cdot(\boldsymbol{x}'-\boldsymbol{x})}e^{iz(\boldsymbol{\kappa}-\boldsymbol{\kappa}')\cdot\boldsymbol{\kappa}''/k}\\ &\quad\times\mathcal{V}^R(1,l(\boldsymbol{\kappa}+\boldsymbol{\kappa}')/2,l(\boldsymbol{\kappa}-\boldsymbol{\kappa}'),l\boldsymbol{\kappa}'';\alpha(k,L),\beta(k,L))\mathrm{d}\boldsymbol{\kappa}'',\end{aligned}$$

with $\alpha(k,z)=z/(kl^2)$ scaling the diffraction strength and $\beta(k,z)=z\sigma^2k^2l/4$ characterizing the strength of forward scattering. We then find that

$$\begin{aligned}\mathcal{H}(\boldsymbol{x},\boldsymbol{y})&=\frac{1}{(2\pi)^{2d}}\left(\frac{l}{2}\right)^d\int\int e^{i\boldsymbol{\kappa}''\cdot((\boldsymbol{x}'+\boldsymbol{x}'')/2-\boldsymbol{x})}e^{iL(\boldsymbol{\kappa}-\boldsymbol{\kappa}')\cdot\boldsymbol{\kappa}''/k_0}\\ &\quad\times\mathcal{V}^R(1,l(\boldsymbol{\kappa}+\boldsymbol{\kappa}')/2,l(\boldsymbol{\kappa}-\boldsymbol{\kappa}'),l\boldsymbol{\kappa}'';\ \alpha(k_0,L),\beta(k_0,L))\mathrm{d}\boldsymbol{\kappa}''\\ &\quad\times e^{i(\boldsymbol{\kappa}\cdot\boldsymbol{y}+\boldsymbol{\kappa}'\cdot(\boldsymbol{x}'-\boldsymbol{x}''))}\mathrm{d}\boldsymbol{\kappa}\,\mathrm{d}\boldsymbol{\kappa}'e^{-\frac{|\boldsymbol{x}'|^2+|\boldsymbol{x}''|^2}{2r_0^2}}e^{ik_0\boldsymbol{\theta}\cdot(\boldsymbol{x}'-\boldsymbol{x}'')}\,\mathrm{d}\boldsymbol{x}'\,\mathrm{d}\boldsymbol{x}''\\ &=\left(\frac{1}{2(2\pi l)^2}\right)^d\int\int e^{i\boldsymbol{s}\cdot((\boldsymbol{x}'+\boldsymbol{x}'')/2-\boldsymbol{x})/l}e^{iL\boldsymbol{r}\cdot\boldsymbol{s}/(k_0l^2)}\\ &\quad\times\mathcal{V}^R(1,\boldsymbol{q},\boldsymbol{r},\boldsymbol{s};\alpha(k_0,L),\beta(k_0,L))e^{i((\boldsymbol{q}+\boldsymbol{r}/2)\cdot\boldsymbol{y}+(\boldsymbol{q}-\boldsymbol{r}/2)\cdot(\boldsymbol{x}'-\boldsymbol{x}''))/l}\,\mathrm{d}\boldsymbol{q}\,\mathrm{d}\boldsymbol{r}\,\mathrm{d}\boldsymbol{s}\\ &\quad\times e^{-\frac{|\boldsymbol{x}'|^2+|\boldsymbol{x}''|^2}{2r_0^2}}e^{ik_0\boldsymbol{\theta}\cdot(\boldsymbol{x}'-\boldsymbol{x}'')}\,\mathrm{d}\boldsymbol{x}'\,\mathrm{d}\boldsymbol{x}''.\end{aligned}$$

Integrating in $\boldsymbol{x}'$, $\boldsymbol{x}''$ we get

$$\begin{aligned}\mathcal{H}(\boldsymbol{x},\boldsymbol{y})&=\left(\frac{r_0^2}{4\pi l^2}\right)^d\int\int e^{-i\boldsymbol{s}\cdot\boldsymbol{x}/l}e^{i\alpha(k_0,L)\boldsymbol{r}\cdot\boldsymbol{s}}e^{i(\boldsymbol{q}+\boldsymbol{r}/2)\cdot\boldsymbol{y}/l}\\ &\quad\times\mathcal{V}^R(1,\boldsymbol{q},\boldsymbol{r},\boldsymbol{s};\alpha(k_0,L),\beta(k_0,L))e^{-r_0^2\left(|k_0\boldsymbol{\theta}+(\boldsymbol{q}-\boldsymbol{r}/2)/l|^2+|\boldsymbol{s}/(2l)|^2\right)}\,\mathrm{d}\boldsymbol{q}\,\mathrm{d}\boldsymbol{r}\,\mathrm{d}\boldsymbol{s}.\end{aligned}$$

We change variables of integration, $\boldsymbol{r}\mapsto\boldsymbol{r}+2\boldsymbol{q}$, $\boldsymbol{s}\mapsto\boldsymbol{s}/(2\alpha(k_0,L))$, and get

$$\begin{aligned}\mathcal{H}(\boldsymbol{x},\boldsymbol{y})&=\left(\frac{r_0^2}{8\pi l^2\alpha(k_0,L)}\right)^d\int\int e^{-i\boldsymbol{s}\cdot\boldsymbol{x}/(2l\alpha(k_0,L))}e^{i(\boldsymbol{q}+\boldsymbol{r}/2)\cdot\boldsymbol{s}}e^{i(2\boldsymbol{q}+\boldsymbol{r}/2)\cdot\boldsymbol{y}/l}\\ &\quad\times\mathcal{V}^R\left(1,\boldsymbol{q},\boldsymbol{r}+2\boldsymbol{q},\frac{\boldsymbol{s}}{2\alpha(k_0,L)};\alpha(k_0,L),\beta(k_0,L)\right)\\ &\quad\times e^{-r_0^2\left(|k_0\boldsymbol{\theta}-\boldsymbol{r}/(2l)|^2+|\boldsymbol{s}/(4\alpha(k_0,L)l)|^2\right)}\,\mathrm{d}\boldsymbol{q}\,\mathrm{d}\boldsymbol{r}\,\mathrm{d}\boldsymbol{s}.\end{aligned}$$

Next, we use Lemma 2.1 to obtain

$$\begin{aligned}\mathcal{H}(\boldsymbol{x},\boldsymbol{y})&=\left(\frac{r_0^2}{16\pi^2l^2\alpha(k_0,L)}\right)^d\int\int e^{-i\boldsymbol{s}\cdot\boldsymbol{x}/(2l\alpha(k_0,L))}e^{i(\boldsymbol{r}/2+\boldsymbol{q})\cdot\boldsymbol{s}}e^{i(2\boldsymbol{q}+\boldsymbol{r}/2)\cdot\boldsymbol{y}/l}\\ &\quad\times e^{-i\boldsymbol{q}\cdot\boldsymbol{u}}e^{\beta(k_0,L)\int_{-1}^1 D_0(\frac{\boldsymbol{u}}{2}+\frac{\boldsymbol{s}}{2\zeta})-D_0(\boldsymbol{0})\mathrm{d}\zeta}e^{-r_0^2\left(|k_0\boldsymbol{\theta}-\boldsymbol{r}/(2l)|^2+|\boldsymbol{s}/(4\alpha(k_0,L)l)|^2\right)}\,\mathrm{d}\boldsymbol{q}\,\mathrm{d}\boldsymbol{r}\,\mathrm{d}\boldsymbol{s}\,\mathrm{d}\boldsymbol{u}.\end{aligned}$$

Integrating in $\boldsymbol{q}$ and evaluating the associated Dirac function, we get

$$\mathcal{H}(\boldsymbol{x},\boldsymbol{y}) = \left(\frac{r_0^2}{8\pi l^2\alpha(k_0,L)}\right)^d \int\int e^{-i\boldsymbol{s}\cdot\boldsymbol{x}/(2l\alpha(k_0,L))} e^{i\boldsymbol{r}\cdot(\boldsymbol{s}+\boldsymbol{y}/l)/2} \times e^{2\beta(k_0,L)\int_0^1 D_0(\frac{\boldsymbol{y}}{l}+\boldsymbol{s}\zeta)-D_0(\boldsymbol{0})\mathrm{d}\zeta} \times e^{-r_0^2\left(|k_0\boldsymbol{\theta}-\boldsymbol{r}/(2l)|^2+|\boldsymbol{s}/(4\alpha(k_0,L)l)|^2\right)}\,\mathrm{d}\boldsymbol{r}\,\mathrm{d}\boldsymbol{s}.$$

Integrating in $\boldsymbol{r}$ yields

$$\mathcal{H}(\boldsymbol{x},\boldsymbol{y}) = \left(\frac{r_0}{4\sqrt{\pi}l\alpha(k_0,L)}\right)^d \int e^{-i\boldsymbol{s}\cdot\boldsymbol{x}/(2l\alpha(k_0,L))} e^{ik_0\boldsymbol{\theta}\cdot(\boldsymbol{y}+\boldsymbol{s}l)} e^{-\frac{|\boldsymbol{y}+\boldsymbol{s}l|^2}{4r_0^2}} \times e^{-\left|\frac{r_0\boldsymbol{s}}{4\alpha(k_0,L)l}\right|^2} e^{2\beta(k_0,L)\int_0^1 D_0(\frac{\boldsymbol{y}}{l}+\boldsymbol{s}\zeta)-D_0(\boldsymbol{0})\mathrm{d}\zeta}\,\mathrm{d}\boldsymbol{s}.$$

Using that $D(\boldsymbol{x}) = \sigma^2 l D_0(\boldsymbol{x}/l)$ we can rewrite the right-hand side as

$$\begin{aligned}\mathcal{H}(\boldsymbol{x},\boldsymbol{y}) &= \left(\frac{r_0}{2\sqrt{\pi}}\right)^d \int e^{-i\boldsymbol{\eta}\cdot\boldsymbol{x}} e^{ik_0\boldsymbol{\theta}\cdot(\boldsymbol{y}+2\boldsymbol{\eta}L/k_0)} e^{-\frac{|\boldsymbol{y}+2\boldsymbol{\eta}L/k_0|^2}{4r_0^2}} e^{-\frac{|r_0\boldsymbol{\eta}|^2}{4}} e^{\frac{k_0^2}{4}\int_0^{2L} D(\boldsymbol{y}+\frac{\boldsymbol{\eta}\zeta}{k_0})-D(\boldsymbol{0})\mathrm{d}\zeta}\,\mathrm{d}\boldsymbol{\eta}\\ &\simeq \left(\frac{r_0}{2\sqrt{\pi}}\right)^d \int e^{-i\boldsymbol{\eta}\cdot\boldsymbol{x}} e^{ik_0\boldsymbol{\theta}\cdot(\boldsymbol{y}+2\boldsymbol{\eta}L/k_0)} e^{-\frac{|\boldsymbol{y}|^2}{4r_0^2}} e^{-\frac{|r_0\boldsymbol{\eta}|^2}{4}} e^{\frac{k_0^2}{4}\int_0^{2L} D(\boldsymbol{y}+\frac{\boldsymbol{\eta}\zeta}{k_0})-D(\boldsymbol{0})\mathrm{d}\zeta}\,\mathrm{d}\boldsymbol{\eta},\end{aligned}$$

where we used that $L/(k_0 r_0^2) \ll 1$. Substituting this result into (65) gives (43).

Appendix 2. Wigner asymptotics

We cast the Wigner distribution in a suitable dimensionless form and present an asymptotic approximation valid in the regime given by the scaling relation in Assumption (c). We state the result here for completeness; see [3] for a comprehensive discussion.

We consider the following Fourier transform V^R of the Wigner distribution W_k^R:

$$W_k^R(z,\boldsymbol{x},\boldsymbol{x}',\boldsymbol{\kappa},\boldsymbol{\kappa}') = \frac{1}{(2\pi)^d}\int V_k^R\left(z,\frac{\boldsymbol{\kappa}+\boldsymbol{\kappa}'}{2},\boldsymbol{\kappa}-\boldsymbol{\kappa}',\boldsymbol{\kappa}''\right)e^{i\boldsymbol{\kappa}''\cdot(\boldsymbol{x}'-\boldsymbol{x})}\mathrm{d}\boldsymbol{\kappa}'', \tag{66}$$

which we introduce because the stationary maps that we will identify in Lemma 2.1, in the asymptotic regime $\alpha\to\infty$, have simple representations in this new frame. Note also that this ansatz incorporates the fact that W_k^R does not depend on $\boldsymbol{x}+\boldsymbol{x}'$, only on $\boldsymbol{x}-\boldsymbol{x}'$, $\boldsymbol{\kappa}$, and $\boldsymbol{\kappa}'$, which follows from the stationarity of the random medium. The Fourier-transformed kernel $V_k^R(z,\boldsymbol{\kappa},\boldsymbol{\kappa}',\boldsymbol{\kappa}'')$ satisfies

$$V_k^R(0,\boldsymbol{\kappa},\boldsymbol{\kappa}',\boldsymbol{\kappa}'') = \mathcal{R}_0^2(\pi l)^d e^{\frac{i}{4}\boldsymbol{\kappa}'\cdot\boldsymbol{\kappa}''}\mathcal{V}^R(1,\boldsymbol{\kappa}l,\boldsymbol{\kappa}'l,\boldsymbol{\kappa}''l;\alpha(k,L),\beta(k,L)), \tag{67}$$

where $(\mathcal{V}^R(\zeta,\boldsymbol{q},\boldsymbol{r},\boldsymbol{s};\alpha,\beta))_{\zeta\in[0,\ 1]}$ is the solution of the dimensionless system

$$\begin{aligned}\frac{\partial\mathcal{V}^R}{\partial\zeta} = \frac{\beta}{(2\pi)^d}\int \hat{D}_0(\boldsymbol{u})\Bigg[&\mathcal{V}^R\left(\zeta,\boldsymbol{q}-\frac{1}{2}\boldsymbol{u},\boldsymbol{r}-\boldsymbol{u},\boldsymbol{s}\right)e^{-i\alpha\boldsymbol{s}\cdot\boldsymbol{u}\zeta}\\ &+\mathcal{V}^R\left(\zeta,\boldsymbol{q}-\frac{1}{2}\boldsymbol{u},\boldsymbol{r}+\boldsymbol{u},\boldsymbol{s}\right)e^{i\alpha\boldsymbol{s}\cdot\boldsymbol{u}\zeta}+\mathcal{V}^R\left(\zeta,\boldsymbol{q}-\frac{1}{2}\boldsymbol{u},\boldsymbol{r},\boldsymbol{s}-\boldsymbol{u}\right)e^{-i\alpha\boldsymbol{r}\cdot\boldsymbol{u}\zeta}\\ &+\mathcal{V}^R\left(\zeta,\boldsymbol{q}-\frac{1}{2}\boldsymbol{u},\boldsymbol{r},\boldsymbol{s}+\boldsymbol{u}\right)e^{i\alpha\boldsymbol{r}\cdot\boldsymbol{u}\zeta}-2\mathcal{V}^R(\zeta,\boldsymbol{\kappa},\boldsymbol{r},\boldsymbol{s})\\ &-\mathcal{V}^R\left(\zeta,\boldsymbol{q}-\frac{1}{2}\boldsymbol{u},\boldsymbol{r}-\boldsymbol{u},\boldsymbol{s}+\boldsymbol{u}\right)e^{i\alpha[(\boldsymbol{r}-\boldsymbol{s})\cdot\boldsymbol{u}-|\boldsymbol{u}|^2]\zeta}\\ &-\mathcal{V}^R\left(\zeta,\boldsymbol{q}-\frac{1}{2}\boldsymbol{u},\boldsymbol{r}-\boldsymbol{u},\boldsymbol{s}-\boldsymbol{u}\right)e^{-i\alpha[(\boldsymbol{r}+\boldsymbol{s})\cdot\boldsymbol{u}+|\boldsymbol{u}|^2]\zeta}\Bigg]\mathrm{d}\boldsymbol{u},\end{aligned} \tag{68}$$

starting from $\mathcal{V}^R(\zeta=0,\boldsymbol{q},\boldsymbol{r},\boldsymbol{s};\alpha,\beta)=\delta(\boldsymbol{q})$. Recall that $\alpha(k,L)=L/(kl^2)$ and $\beta(k,L)=\sigma^2k^2lL/4$.

The rapid transverse variations regime is particularly interesting to study because W_k^R has a multi-scale behavior. In (68) this regime gives rise to rapid phases and this allows us to identify a simplified description and the multiscale behavior strongly influences the correlations. The following lemma describes the asymptotic behavior of $\mathcal{V}^R$ as $\alpha \to \infty$. The presence of singular layers at $\boldsymbol{r}=\boldsymbol{0}$ and at $\boldsymbol{s}=\boldsymbol{0}$ requires particular attention and is responsible for instance for the enhanced backscattering phenomenon [3] (corresponding to part (3) in Lemma 2.1). In general (part (1) in Lemma 2.1) the Fourier-transformed operator decays exponentially according to the parameter $\beta D_0(\boldsymbol{0})$ corresponding to the total scattering cross-section. This decay follows from a partial loss of coherence by random forward scattering. However, as articulated in parts (2) and (3) of the lemma below the coupling of wave modes depends on the full medium autocorrelation function if we look at nearby specular reflection and small spatial offset frequencies. We have [3]

Lemma 2.1

(1) *For any* $\boldsymbol{r}\neq\boldsymbol{0}$, $\boldsymbol{s}\neq\boldsymbol{0}$:

$$\mathcal{V}^R(\zeta,\boldsymbol{q},\boldsymbol{r},\boldsymbol{s};\alpha,\beta) \overset{\alpha\to\infty}{\longrightarrow} \delta(\boldsymbol{q})e^{-2\beta D_0(\boldsymbol{0})\zeta}. \tag{69}$$

(2) *For any* $\boldsymbol{s}\neq\boldsymbol{0}$ *we have* $\mathcal{V}^R(\zeta,\boldsymbol{q},\frac{\boldsymbol{r}}{\alpha},\boldsymbol{s};\alpha,\beta) \overset{\alpha\to\infty}{\longrightarrow} \mathcal{V}_{\boldsymbol{r}}^R(\zeta,\boldsymbol{q};\beta)$ *where* $\mathcal{V}_{\boldsymbol{r}}^R(\zeta,\boldsymbol{q};\beta)$ *is the solution of*

$$\frac{\partial \mathcal{V}_{\boldsymbol{r}}^R}{\partial\zeta} = \frac{2\beta}{(2\pi)^d}\int \hat{D}_0(\boldsymbol{u})\left[\mathcal{V}_{\boldsymbol{r}}^R\left(\zeta,\boldsymbol{q}-\frac{1}{2}\boldsymbol{u}\right)\cos(\boldsymbol{r}\cdot\boldsymbol{u}\zeta) - \mathcal{V}_{\boldsymbol{r}}^R(\zeta,\boldsymbol{q})\right]\mathrm{d}\boldsymbol{u}, \tag{70}$$

and is given explicitly by

$$\mathcal{V}_{\boldsymbol{r}}^R(\zeta,\boldsymbol{q};\beta) = \frac{1}{(2\pi)^d}\int e^{-i\boldsymbol{q}\cdot\boldsymbol{u}}e^{\beta\int_0^\zeta D_0(\frac{\boldsymbol{u}}{2}+\boldsymbol{r}\zeta')+D_0(\frac{\boldsymbol{u}}{2}-\boldsymbol{r}\zeta')-2D_0(\boldsymbol{0})\mathrm{d}\zeta'}\,\mathrm{d}\boldsymbol{u}. \tag{71}$$

Similarly, for any $\boldsymbol{r}\neq\boldsymbol{0}$ *we have* $\mathcal{V}^R(\zeta,\boldsymbol{q},\boldsymbol{r},\frac{\boldsymbol{s}}{\alpha};\alpha,\beta) \overset{\alpha\to\infty}{\longrightarrow} \mathcal{V}_{\boldsymbol{s}}^R(\zeta,\boldsymbol{q};\beta)$.

(3) *For any* $\boldsymbol{r}$ *and* $\boldsymbol{s}$ *we have*

$$\mathcal{V}^R\left(\zeta,\boldsymbol{q},\frac{\boldsymbol{r}}{\alpha},\frac{\boldsymbol{s}}{\alpha};\alpha,\beta\right) \overset{\alpha\to\infty}{\longrightarrow} \mathcal{V}_{\boldsymbol{r}}^R(\zeta,\boldsymbol{q};\beta) + \mathcal{V}_{\boldsymbol{s}}^R(\zeta,\boldsymbol{q};\beta) - \delta(\boldsymbol{q})e^{-2\beta D_0(\boldsymbol{0})\zeta}. \tag{72}$$

We next discuss the modification of the above result that follows from using a diffusive interface as introduced in Section 8.2. Under these conditions, the initial condition for the Wigner distribution is $W^R(z=L,\boldsymbol{x},\boldsymbol{x}',\boldsymbol{q},\boldsymbol{q}') = R_0^2\delta(\boldsymbol{x}-\boldsymbol{x}')\hat{\psi}(\boldsymbol{q}+\boldsymbol{q}')$. The associated initial condition for $\mathcal{V}^R$ is $\mathcal{V}^R(\zeta=0,\boldsymbol{q},\boldsymbol{r},\boldsymbol{s}) = (\pi l)^{-d}\hat{\psi}(2\boldsymbol{q}/l)$. Lemma 2.1 is then modified as follows

Lemma 2.2

(1) *For any* $\boldsymbol{r}\neq\boldsymbol{0}$, $\boldsymbol{s}\neq\boldsymbol{0}$:

$$\mathcal{V}^R(\zeta,\boldsymbol{q},\boldsymbol{r},\boldsymbol{s};\alpha,\beta) \overset{\alpha\to\infty}{\longrightarrow} (\pi l)^{-d}\hat{\psi}(2\boldsymbol{q}/l)e^{-2\beta D_0(\boldsymbol{0})\zeta}. \tag{73}$$

(2) *For any* $\boldsymbol{s}\neq\boldsymbol{0}$ *we have* $\mathcal{V}^R(\zeta,\boldsymbol{q},\frac{\boldsymbol{r}}{\alpha},\boldsymbol{s};\alpha,\beta) \overset{\alpha\to\infty}{\longrightarrow} \mathcal{V}_{\boldsymbol{r}}^R(\zeta,\boldsymbol{q};\beta)$ *where* $\mathcal{V}_{\boldsymbol{r}}^R(\zeta,\boldsymbol{q};\beta)$ *is solution of*

$$\frac{\partial \mathcal{V}_{\boldsymbol{r}}^R}{\partial\zeta} = \frac{2\beta}{(2\pi)^d}\int \hat{D}_0(\boldsymbol{u})\left[\mathcal{V}_{\boldsymbol{r}}^R\left(\zeta,\boldsymbol{q}-\frac{1}{2}\boldsymbol{u}\right)\cos(\boldsymbol{r}\cdot\boldsymbol{u}\zeta) - \mathcal{V}_{\boldsymbol{r}}^R(\zeta,\boldsymbol{q})\right]\mathrm{d}\boldsymbol{u}, \tag{74}$$

and is given explicitly by

$$\mathcal{V}_{\boldsymbol{r}}^R(\zeta,\boldsymbol{q};\beta) = \frac{1}{(2\pi)^d}\int \psi\left(\frac{l\boldsymbol{u}}{2}\right)e^{-i\boldsymbol{q}\cdot\boldsymbol{u}}e^{\beta\int_0^\zeta D_0(\frac{\boldsymbol{u}}{2}+\boldsymbol{r}\zeta')+D_0(\frac{\boldsymbol{u}}{2}-\boldsymbol{r}\zeta')-2D_0(\boldsymbol{0})\mathrm{d}\zeta'}\,\mathrm{d}\boldsymbol{u}. \tag{75}$$

Similarly, for any $\boldsymbol{r}\neq\boldsymbol{0}$ *we have* $\mathcal{V}^R(\zeta,\boldsymbol{q},\boldsymbol{r},\frac{\boldsymbol{s}}{\alpha};\alpha,\beta) \overset{\alpha\to\infty}{\longrightarrow} \mathcal{V}_{\boldsymbol{s}}^R(\zeta,\boldsymbol{q};\beta)$.

(3) *For any* $\boldsymbol{r}$ *and* $\boldsymbol{s}$ *we have*

$$\mathcal{V}^R\Big(\zeta, \boldsymbol{q}, \frac{\boldsymbol{r}}{\alpha}, \frac{\boldsymbol{s}}{\alpha}; \alpha, \beta\Big) \overset{\alpha\to\infty}{\longrightarrow} \mathcal{V}^R_{\boldsymbol{r}}(\zeta, \boldsymbol{q}; \beta) + \mathcal{V}^R_{\boldsymbol{s}}(\zeta, \boldsymbol{q}; \beta) - (\pi l)^{-d}\hat{\psi}(2\boldsymbol{q}/l)e^{-2\beta D_0(\boldsymbol{0})\zeta}. \tag{76}$$

Proof In case (1), the rapid phases cancel the contributions of all but the term $\mathcal{V}^R(\zeta, \boldsymbol{q}, \boldsymbol{r}, \boldsymbol{s})$ in (68), and we get

$$\frac{\partial \mathcal{V}^R}{\partial \zeta} = -2\frac{\beta}{(2\pi)^d}\int \hat{D}_0(\boldsymbol{u})\mathcal{V}^R \mathrm{d}\boldsymbol{u} = -2\beta D_0(\boldsymbol{0})\mathcal{V}^R,$$

which gives (69) and (73) in view of the corresponding initial conditions. In case (2), we obtain in the limit $\alpha \to \infty$ the simplified system

$$\frac{\partial \mathcal{V}^R_{\boldsymbol{r}}}{\partial \zeta} = \frac{\beta}{(2\pi)^d}\int \hat{D}_0(\boldsymbol{u})\Big[\mathcal{V}^R_{\boldsymbol{r}}\Big(\zeta, \boldsymbol{q} - \frac{1}{2}\boldsymbol{u}, \boldsymbol{s} - \boldsymbol{u}\Big)e^{-i\boldsymbol{r}\cdot\boldsymbol{u}\zeta} + \mathcal{V}^R_{\boldsymbol{r}}\Big(\zeta, \boldsymbol{q} - \frac{1}{2}\boldsymbol{u}, \boldsymbol{s} + \boldsymbol{u}\Big)e^{i\boldsymbol{r}\cdot\boldsymbol{u}\zeta} - 2\mathcal{V}^R_{\boldsymbol{r}}(\zeta, \boldsymbol{q}, \boldsymbol{s})\Big]\mathrm{d}\boldsymbol{u}.$$

We then Fourier transform this equation in $\boldsymbol{q}$ and $\boldsymbol{s}$, and we obtain that the solution does not depend on $\boldsymbol{s}$, that it satisfies (70), and that it is given by (71) and (75).

In case (3) we obtain the simplified system for $\mathcal{V}^R_{\boldsymbol{r},\boldsymbol{s}}(\zeta, \boldsymbol{q}) = \lim_{\alpha\to\infty}\mathcal{V}^R\big(\zeta, \boldsymbol{q}, \frac{\boldsymbol{r}}{\alpha}, \frac{\boldsymbol{s}}{\alpha}\big)$:

$$\frac{\partial \mathcal{V}^R_{\boldsymbol{r},\boldsymbol{s}}}{\partial \zeta} = \frac{2\beta}{(2\pi)^d}\int \hat{D}_0(\boldsymbol{u})\Big[\mathcal{V}^R_{\boldsymbol{s}}\Big(\zeta, \boldsymbol{q} - \frac{1}{2}\boldsymbol{u}\Big)\cos(\boldsymbol{s}\cdot\boldsymbol{u}\zeta) + \mathcal{V}^R_{\boldsymbol{r}}\Big(\zeta, \boldsymbol{q} - \frac{1}{2}\boldsymbol{u}\Big)\cos(\boldsymbol{r}\cdot\boldsymbol{u}\zeta) - \mathcal{V}^R_{\boldsymbol{r},\boldsymbol{s}}(\zeta, \boldsymbol{q})\Big]\mathrm{d}\boldsymbol{u}.$$

Using Equation (70) satisfied by $\mathcal{V}^R_{\boldsymbol{s}}$ and $\mathcal{V}^R_{\boldsymbol{r}}$, we get

$$\frac{\partial \mathcal{V}^R_{\boldsymbol{r},\boldsymbol{s}}}{\partial \zeta} = \frac{\partial \mathcal{V}^R_{\boldsymbol{r}}}{\partial \zeta} + \frac{\partial \mathcal{V}^R_{\boldsymbol{s}}}{\partial \zeta} + 2\beta D_0(\boldsymbol{0})\Big[\mathcal{V}^R_{\boldsymbol{r}} + \mathcal{V}^R_{\boldsymbol{s}} - \mathcal{V}^R_{\boldsymbol{r},\boldsymbol{s}}\Big],$$

which yields (72) and (76). □

Appendix 3. Enhanced backscattered intensity

We derive result (49). Using (48) we first find that

$$\lim_{\varepsilon\to 0}\mathbb{E}\Big[\big|\widetilde{v}_1^\varepsilon(s, \boldsymbol{\kappa}_0)\big|^2\Big] = \mathcal{R}_0^2|f_0^\delta(s)|^2 I^R(\boldsymbol{\kappa}_0),$$

for

$$I^R(\boldsymbol{\kappa}_0) = \frac{1}{\mathcal{R}_0^2}\int\int \mathbb{E}\Big[\widehat{\boldsymbol{\mathcal{R}}}^\varepsilon(k_0, 0, \boldsymbol{\kappa}_0 - k_0\boldsymbol{\theta}, \boldsymbol{\kappa}_1' + k_0\boldsymbol{\theta}) \times \overline{\widehat{\boldsymbol{\mathcal{R}}}^\varepsilon(k_0, 0, \boldsymbol{\kappa}_0 - k_0\boldsymbol{\theta}, \boldsymbol{\kappa}_2' + k_0\boldsymbol{\theta})}\Big]\hat{g}_{\mathrm{inc}}(\boldsymbol{\kappa}_1')\overline{\hat{g}_{\mathrm{inc}}(\boldsymbol{\kappa}_2')}\mathrm{d}\boldsymbol{\kappa}_1'\mathrm{d}\boldsymbol{\kappa}_2'.$$

In view of (28) and (63) we have

$$\begin{aligned}\mathbb{E}\Big[\widehat{\boldsymbol{\mathcal{R}}}^\varepsilon(k_0, 0, \boldsymbol{\kappa}_0, \boldsymbol{\kappa}_1')\overline{\widehat{\boldsymbol{\mathcal{R}}}^\varepsilon(k_0, 0, \boldsymbol{\kappa}_0, \boldsymbol{\kappa}_2')}\Big] &= \frac{1}{(2\pi)^{4d}}\int\int e^{-i(\boldsymbol{x}\cdot\boldsymbol{\kappa}_0 - \boldsymbol{x}'\cdot\boldsymbol{\kappa}_1')}e^{i(\tilde{\boldsymbol{x}}\cdot\boldsymbol{\kappa}_0 - \tilde{\boldsymbol{x}}'\cdot\boldsymbol{\kappa}_2')} \\ &\times e^{i\boldsymbol{q}\cdot(\boldsymbol{x}-\tilde{\boldsymbol{x}})}e^{i\boldsymbol{q}'\cdot(\boldsymbol{x}'-\tilde{\boldsymbol{x}}')}W^R_{k_0}(0, (\boldsymbol{x}+\tilde{\boldsymbol{x}})/2, (\boldsymbol{x}'+\tilde{\boldsymbol{x}}')/2, \boldsymbol{q}, \boldsymbol{q}')\,\mathrm{d}\boldsymbol{x}\,\mathrm{d}\boldsymbol{x}'\mathrm{d}\tilde{\boldsymbol{x}}\,\mathrm{d}\tilde{\boldsymbol{x}}'\,\mathrm{d}\boldsymbol{q}\,\mathrm{d}\boldsymbol{q}'\end{aligned}$$

$$= \frac{1}{(2\pi)^{4d}} \int\int e^{-i\boldsymbol{\kappa}_0\cdot z} e^{i(\tilde{z}'+z'/2)\cdot\boldsymbol{\kappa}_1'} e^{-i(\tilde{z}'-z'/2)\cdot\boldsymbol{\kappa}_2'} e^{i\boldsymbol{q}\cdot z} e^{i\boldsymbol{q}'\cdot z'} W^R_{k_0}(0,\tilde{z},\tilde{z}',\boldsymbol{q},\boldsymbol{q}')\,\mathrm{d}z\,\mathrm{d}z'\,\mathrm{d}\tilde{z}\,\mathrm{d}\tilde{z}'\,\mathrm{d}\boldsymbol{q}\,\mathrm{d}\boldsymbol{q}'$$

$$= \frac{1}{(2\pi)^{2d}} \int\int e^{i\tilde{z}'\cdot(\boldsymbol{\kappa}_1'-\boldsymbol{\kappa}_2')} \delta(\boldsymbol{q}-\boldsymbol{\kappa}_0)\delta(\boldsymbol{q}'+\boldsymbol{\kappa}_1'/2+\boldsymbol{\kappa}_2'/2) W^R_{k_0}(0,\tilde{z},\tilde{z}',\boldsymbol{q},\boldsymbol{q}')\mathrm{d}\tilde{z}\mathrm{d}\tilde{z}'d\boldsymbol{q}d\boldsymbol{q}'.$$

This gives

$$I^R(\boldsymbol{\kappa}_0) = \frac{1}{(2\pi)^{2d}\mathcal{R}_0^2} \int\int W^R_{k_0}(0,\tilde{z},\tilde{z}',\boldsymbol{\kappa}_0 - k_0\boldsymbol{\theta},\ -(\boldsymbol{\kappa}_1'+\boldsymbol{\kappa}_2')/2 - k_0\boldsymbol{\theta})$$
$$\times\, e^{i\tilde{z}'\cdot(\boldsymbol{\kappa}_1'-\boldsymbol{\kappa}_2')} \hat{g}_{\mathrm{inc}}(\boldsymbol{\kappa}_1')\overline{\hat{g}_{\mathrm{inc}}(\boldsymbol{\kappa}_2')}\mathrm{d}\tilde{z}\mathrm{d}\tilde{z}'\mathrm{d}\boldsymbol{\kappa}_1'\mathrm{d}\boldsymbol{\kappa}_2'.$$

In view of (66) we have

$$\int\int W^R_{k_0}(0,\tilde{z},\tilde{z}',\boldsymbol{\kappa}_0,\ -(\boldsymbol{\kappa}_1'+\boldsymbol{\kappa}_2')/2) e^{i\tilde{z}'\cdot(\boldsymbol{\kappa}_1'-\boldsymbol{\kappa}_2')}\mathrm{d}\tilde{z}\mathrm{d}\tilde{z}'$$
$$= (2\pi)^{\mathrm{d}} V^R(0,(\boldsymbol{\kappa}_0-\boldsymbol{\kappa}_1')/2, \boldsymbol{\kappa}_0+\boldsymbol{\kappa}_1', \mathbf{0})\delta(\boldsymbol{\kappa}_1'-\boldsymbol{\kappa}_2').$$

Then, using (67) we find that

$$I^R(\boldsymbol{\kappa}_0) = (l/2)^d \int \mathcal{V}^R(1, l(\boldsymbol{\kappa}_0-\boldsymbol{\kappa}'-2k_0\boldsymbol{\theta})/2, l(\boldsymbol{\kappa}_0+\boldsymbol{\kappa}'), \mathbf{0}; \alpha(k_0,L), \beta(k_0,L))|\hat{g}_{\mathrm{inc}}(\boldsymbol{\kappa}')|^2\mathrm{d}\boldsymbol{\kappa}'.$$